Researchers Journal of Science and Technology (REJOST)
https://rejost.com.ng

Integrated Qualitative and Quantitative Evaluation of Depositional Environment and Hydrocarbon Prospectivity of the QX Field in Southeastern Niger Delta

Ekiliwo N. Justina and Anietie E. Ekot*

Abstract

Exploration in the Niger Delta has matured over decades, yet predicting reservoir quality in newly discovered marginal fields remains uncertain due to persistent subsurface heterogeneity and facies variability. In fields like QX, this uncertainty translates into real investment risk, largely because many existing studies rely on either petrophysical or stratigraphic interpretations in isolation. This study addresses this gap by integrating seismic data, well logs, and sequence stratigraphic frameworks into a unified qualitative–quantitative workflow aimed at improving depositional interpretation and hydrocarbon prediction. Three reservoirs (RES1, RES2, and RES3) were identified and characterized across the field. The combined petrophysical and sequence stratigraphic analysis reveals a progressive depositional architecture, with RES1 and RES2 formed within channelized shoreface systems, while RES3 reflects a lower shoreface setting. Two third-order depositional sequences and their associated system tracts were delineated, establishing a clear stratigraphic linkage from RES3 at the base to RES1 at the top. This integrated approach not only constrains facies distribution but also improves confidence in reservoir continuity and fluid prediction. Reservoir quality indicators show favourable conditions, with net-to-gross values of 69.25–84.75%, porosity ranging from 19.50–25%, shale volume between 12.20–30.75%, and water saturation of 27.94–41.75%. Permeability values (59.68–152.51 mD) further support good reservoir deliverability. Volumetric estimates derived from both deterministic and simplified probabilistic methods provide a more balanced assessment of uncertainty, yielding STOIIP values of 6.13 MMSTB (P50) for RES1 and 58.27 MMSTB (P50) for RES3, alongside GIIP estimates of 2.66 BCF and 9.54 BCF for RES1 and RES2, respectively. Notably, RES2 is interpreted as a gas-bearing unit sandwiched between oil-bearing RES1 and RES3. In all, the QX Field is estimated to contain approximately 64.40 MMSTB of oil and 12.20 BCF of gas. Beyond these volumes, the study demonstrates that integrating depositional architecture with quantitative petrophysical evaluation significantly reduces uncertainty in reservoir prediction. This has practical implications for decision-making in marginal field development, offering a more reliable basis for reserve estimation, risk reduction, and field planning in complex deltaic systems.

✉ Anietie E. Ekot: anietieekot@aksu.edu.ng; anietieekot@gmail.com

Department of Geology, Akwa Ibom State University, Mkpat Enin, Akwa Ibom State, Nigeria.

Keywords: Petrophysics and Geophysics, Sequence stratigraphy, Depositional environment, Hydrocarbon potential, Volumetric Estimation

Article history

Received: February 3, 2026
Received in revised form: March 29, 2026
Accepted for publication: April 12, 2026
Available online: April 16, 2026

1.0 Introduction

Hydrocarbon exploration remains a capital intensive and inherently uncertain venture. Drilling a single exploratory well can cost between six and eight million US dollars, often reaching depths of 10,000 to 12,000 feet. Despite this significant investment, success rates remain low, with only about one or two out of every ten wells drilled in Nigeria yielding hydrocarbons in commercial quantities (Oloruntobi, 1997). This reality highlights the level of financial exposure faced by stakeholders in the oil and gas industry. For most companies, their economic strength is closely tied to the size and reliability of their hydrocarbon reserves, which serve as a key indicator of both current performance and future sustainability.

Given these uncertainties, reducing exploration risk begins with a thorough understanding of subsurface conditions in a prospective field such as the QX Field. One of the most critical steps in this process is the estimation of hydrocarbon volumes, commonly referred to as volumetric estimation. This can be approached using either deterministic or probabilistic methods, both of which are designed to quantify the amount of hydrocarbons present within a reservoir. However, such estimates are not static. They evolve over the life of the field as new data becomes available and as improved techniques for data acquisition and interpretation are introduced. Deterministic approaches rely on available field data such as well logs, seismic records, and core samples to derive reservoir properties (Tearpock and Bischke, 2003). In contrast, probabilistic methods incorporate predictive tools, Monte Carlo statistics, and analog field information to account for uncertainty and variability in reservoir characteristics beyond the sampled locations. Volumetric techniques are used to estimate stock tank oil initially in place or gas initially in place, providing a basis for identifying hydrocarbon accumulation (Dake, 1978). These estimates are derived from key parameters such as reservoir area, thickness, porosity, water saturation, and fluid properties. Recoverable volumes are then determined by applying a recovery factor, which is often based on analog field performance or simulation studies.

Over the years, the integration of seismic interpretation with petrophysical analysis has become a standard practice in reservoir evaluation (Adeoye and Enikauselu, 2009; Aigbedion & Iyayi, 2007; Emujakporue & Faluyi, 2015). In hydrocarbon bearing provinces, particularly in the Niger Delta, a detailed understanding of reservoir properties is essential for effective exploration and development. Reservoir characterization provides valuable insight into parameters such as porosity, permeability, hydrocarbon saturation, fluid distribution, and net sand thickness, all of which are necessary for building a realistic picture of reservoir architecture and performance.

In this study, volumetric estimation is carried out primarily using a deterministic framework, supported by a modified probabilistic approach that represents a simplified form of Monte Carlo simulation. This combined approach is adopted due to limitations in available data, particularly the absence of core measurements. In situations where a full Monte Carlo simulation is not feasible, Downey (2005) recommends the use of a simplified three-point probabilistic estimation applied independently to each reservoir unit. By integrating this approach with deterministic analysis, the study aims to achieve more balanced and reliable estimates for the QX Field. A major gap that motivates this work is the limited application of fully integrated evaluation frameworks in marginal fields within the Niger Delta. Many previous studies have tended to treat depositional environment, petrophysical properties, and structural interpretation as separate components, without adequately exploring how they interact to influence hydrocarbon occurrence and recovery

(Akpan et al., 2020a). This fragmented approach often reduces the reliability of prospect evaluation, especially in smaller or less prolific fields such as QX.

There is also ongoing uncertainty in linking depositional environments directly to reservoir quality. Although facies analysis provides useful insights into sedimentary processes, it does not always translate clearly into predictable petrophysical performance. Variations in grain size, sorting, diagenetic alteration, and subsurface heterogeneity can significantly modify reservoir characteristics, even within similar depositional settings (Castro et al., 2026). This makes it difficult to rely solely on qualitative depositional models without strong quantitative support. Furthermore, many existing volumetric studies still depend heavily on deterministic estimates that produce single value results (Ekong et al., 2025). While useful, such estimates can create a false impression of certainty, particularly in data limited environments where reservoir continuity is not well constrained. Incorporating probabilistic methods that account for uncertainty in parameters such as porosity, saturation, net to gross ratio, and reservoir extent is therefore essential for more realistic resource evaluation (Ekong et al., 2025). This study addresses these gaps by developing a unified workflow that integrates depositional interpretation, petrophysical analysis, and uncertainty based volumetric estimation. By combining qualitative geological understanding with quantitative evaluation techniques, it seeks to provide a more reliable and practical assessment of hydrocarbon prospectivity in the QX Field within the southeastern Niger Delta.

2.0 Location and Geology of the Study Area

The study area Q-X field is in the southeastern region of the Niger Delta basin. It lies within the onshore transition zone of the delta, which is marked by a complex interaction of fluvio-deltaic, delta - front, and pro-deltaic environments. The Niger Delta area is generally found between approximately Latitude 3°N and 6°N, and Longitude 4°E and 8°E. (Figure 1) and the Base Concession Map of QX field is given in Figure 2.

The Niger Delta, one of the world's largest and most prolific deltaic systems, is situated at the apex of the Gulf of Guinea on the West African continental margin. Its immense hydrocarbon reserves and complex geological architecture are fundamentally products of a unique and protracted tectonic evolution intricately linked to the breakup of the supercontinent Gondwana and the opening of the South Atlantic Ocean (Burke,1969). Understanding this tectonic framework is paramount to comprehending the basin's formation, structural styles, sediment infill, and ultimately, its vast petroleum potential. The genesis of the Niger Delta Basin is rooted in the extensional tectonics that commenced in the Late Jurassic, marking the initial stages of the separation of the African and South American continents (Short & Stauble, 1967). This continental rifting established a series of rift basins that would later evolve into the passive continental margins of the South Atlantic. (Whiteman,1982).

The rifting process was characterized by the development of a Y-shaped or "rift-rift-rift" triple junction. Two arms of this triple junction successfully opened to form the South Atlantic Ocean (proto-Atlantic), leading to seafloor spreading and the eventual separation of the continents. The third arm, which failed to develop into a full oceanic basin, extended inland as the Benue trough (Burke et al.,1971). The Benue Trough is a prominent, NE-SW trending rift basin stretching over 1000 km into the African craton. It represents the "failed arm" or "aulacogen" of the triple junction. During the Early Cretaceous (Aptian to Albian), the Benue Trough experienced significant subsidence and received a thick succession of marine and paralic sediments. While not directly part of the active Niger Delta depositional system, its tectonic history significantly influenced the regional stress regime and sediment provenance for the developing delta. Early movements

along major NE-SW trending faults within this failed rift system led to the formation of the Abakaliki Trough, a depocenter for Cretaceous sediments (Uzuakpunwa, 1974). This initial rift phase involved significant crustal stretching and thinning, leading to heat flow and localized volcanism (Doust & Omatsola, 1990). The pre-rift basement, composed primarily of Precambrian metamorphic and igneous rocks of the West African Craton, was fractured and downfaulted, creating the foundational architecture for subsequent sedimentation (Kulke,1995). Following the initial rifting and the onset of seafloor spreading, the tectonic regime transitioned from active extension to passive margin subsidence. This stage was primarily driven by thermal subsidence and load-induced subsidence (Figure 3). As the lithosphere cooled and contracted after the rifting phase, it underwent thermal subsidence, causing a regional down warping of the continental margin (Allen & Allen,2005). This created accommodation space for the immense volumes of clastic sediments that would later form the Niger Delta. The sheer weight of the accumulating sediments (sedimentary load) further contributed to subsidence, creating a feedback loop where deposition led to more subsidence, which in turn allowed for more deposition. (Kulke,1995).

Growth faults, while acting as seals in many cases, can also serve as conduits for hydrocarbon migration from deeper source rocks into shallower Agbada Formation reservoirs. Fault-related fracturing and pressure differences facilitate this movement (Ejedawe,1981). The pervasive gravity tectonics generated abundant structural traps (rollover anticlines, fault closures, mud diapir-related traps) and stratigraphic traps (e.g., pinch-outs against growth faults) within the Agbada Formation.

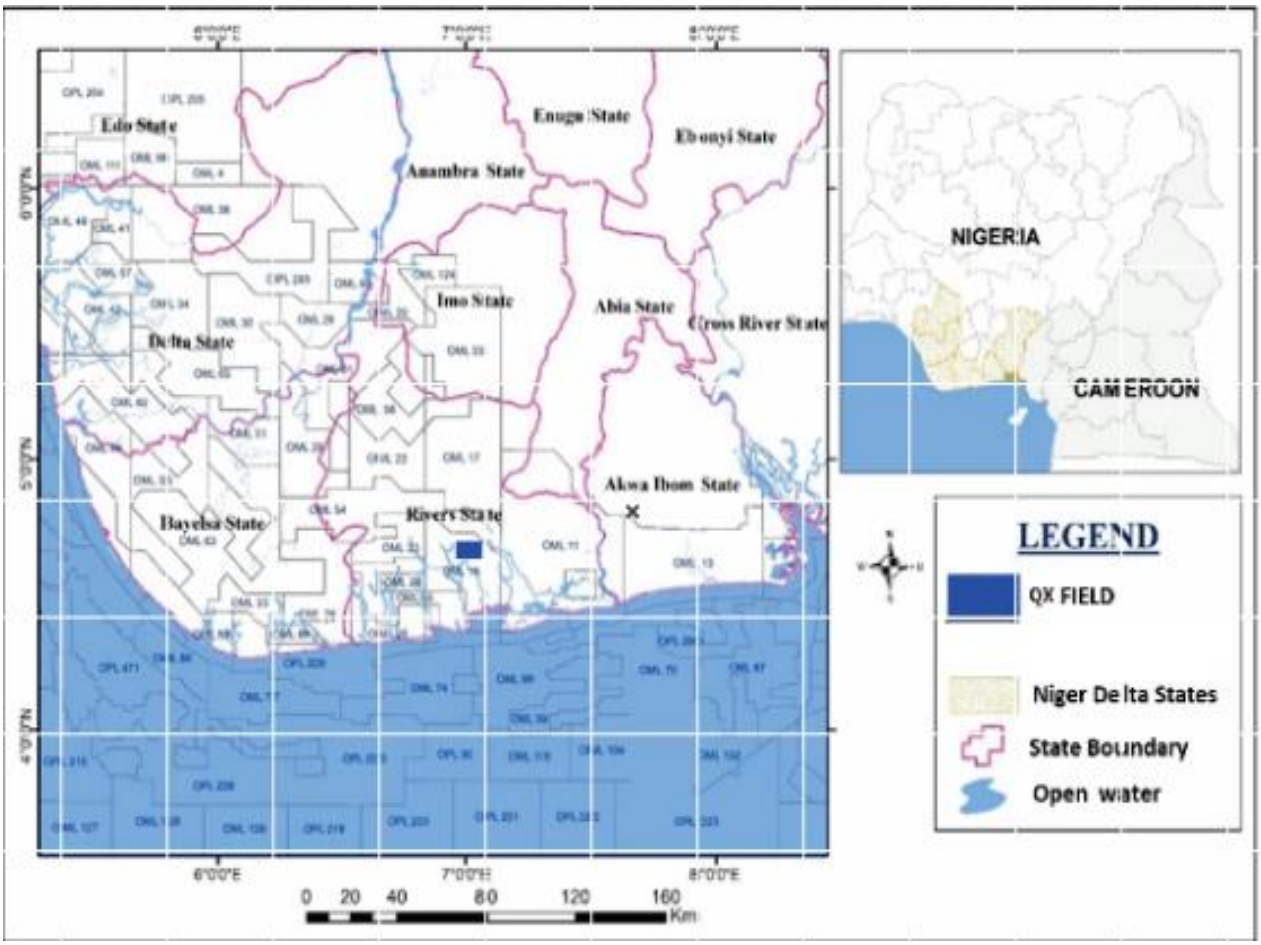

Figure 1: Map showing the Study Area (Modified after Etim et al., 2025)

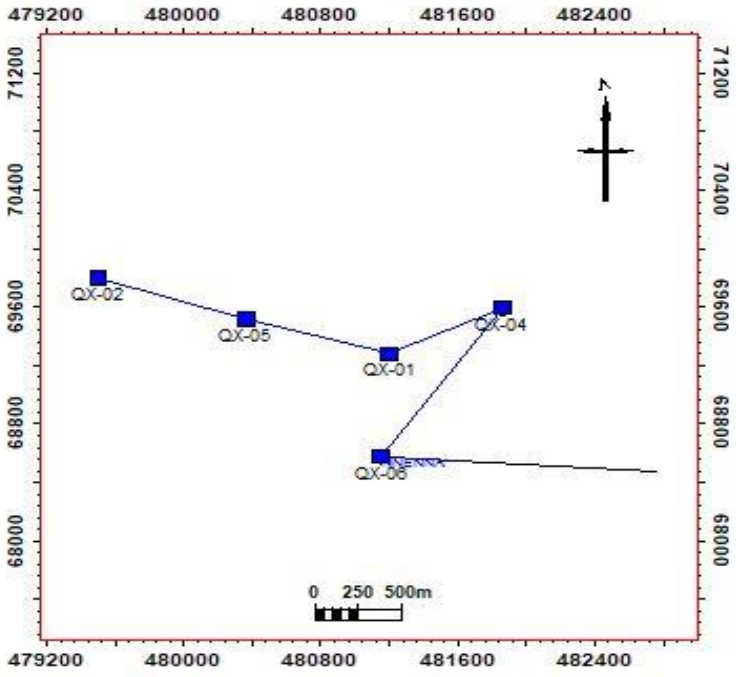

Figure 2: Base Concession Map of QX field showing well trajectory

The interbedded shales within the Agbada serve as excellent seals, (Weber & Daukoru,1975). The continuous nature of the delta's progradation means that hydrocarbon generation, migration, and trap formation are ongoing processes. As the delta progrades, older source rocks are buried deeper and mature, while new traps are continuously being formed and charged. This dynamic "fill-and-spill" model contributes to the basin's sustained productivity (Stacher,1995).

3.0 Materials and Methods

3.1 Datasets and Source

Datasets were obtained from “Q-X” Marginal field reservoirs were obtained from an oil producing company in the Niger Delta with the cooperation of the Nigerian Upstream Petroleum Regulatory Commission (NUPRC).

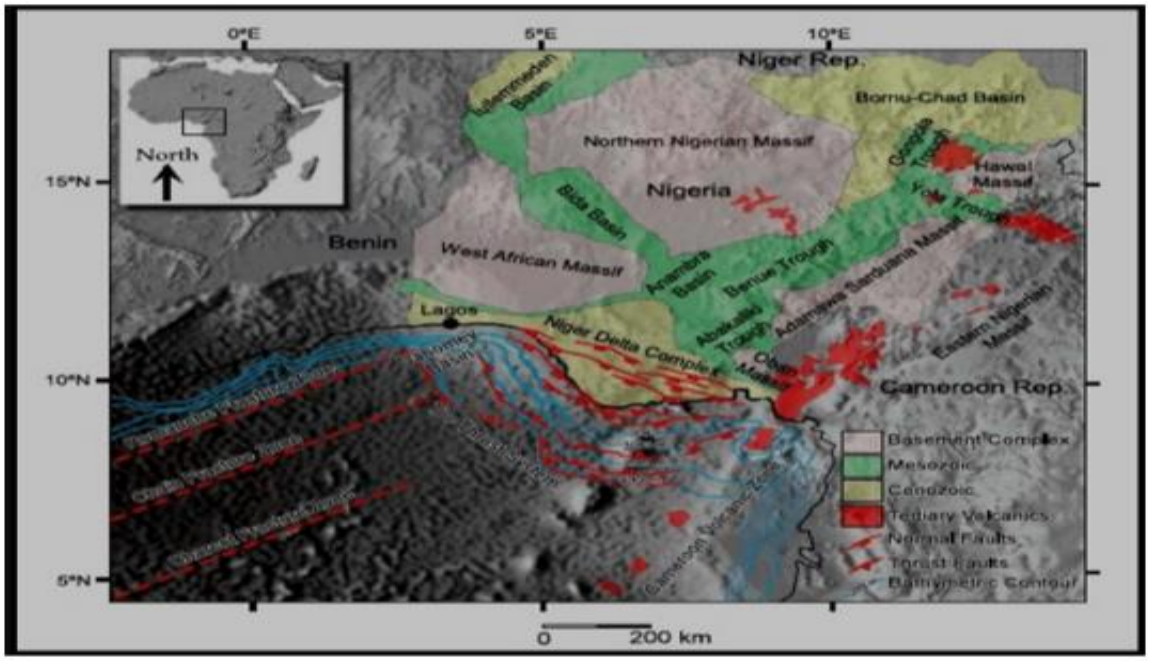

Figure 3: Location Map of the Niger Delta Region Showing the Main Sedimentary Basins and Tectonic feature (Olowokere et al., 2019)

The datasets contained the following: digitized wireline logs in LAS (Log ASCII Standard) check shots, well deviation data, seismic data. The data was analyzed and interpreted using the following software: Schlumberger Petrel, interactive petrophysics, and Microsoft Excel. The wells present and absent according to the available data are summarized in Table 1. The Vintage seismic properties of Q-X Field are also given in Table 2.

Table 1: Well Inventory

Table 2: Vintage seismic properties of Q-X Field

3D SEISMIC DATA	
Format	SEGY – Post Stack
Total Coverage Area	54.78 km^2
Inline Range	5800 – 6200
Cross line Range	1480 – 1700
Sample Interval	4
Time Range	0 – 6000

3.2 Data Loading

The data loading process into Petrel involves several steps to ensure accurate importations into the software environment. Importing well heads and logs is the first step in the data loading procedure. The well head file carries names of the wells, surface position (2D-XY coordinate system), Kelly bushing (Kb), top depth, and bottom depth. This permits well placements to be displayed on the base map (Ekefre et al., 2025). Each well's check shot, deviation, and log data were then imported. The seismic volume was imported using SEG-Y format.

3.3 Well Normalization

Well normalization involved adjusting well log data to a common scale or reference system to ensure consistency and comparability across multiple wells in a reservoir. It is a critical step in subsurface modeling and reservoir characterization, as it helps to remove any inconsistencies caused by varying logging conditions, operational differences, or measurement units. To normalize the wells, the log tracts were scaled from 1-150 API for the gamma ray log, 0.2-2000-ohm meters for the resistivity log, 1.65-2.65g/cm^3 for the density log, 0-0.6 for the neutron porosity log, and 40-140 for the sonic log. Each log track was assigned to a distinct color.

3.4 Reservoir Identification /Well Correlation

This process begins by identifying and correlating formation tops to develop a

chronostratigraphic framework for the field. The wells were all arranged along strike lines West to East which correspond with their location and relative distance to each as observed on the base map. Correlation of the wells was carried out to develop a lateral continuity for each identified horizon (sand interval) across the three wells in the field with the use of the only lithology log available (GR-log) alongside with the resistivity logs to check the fluid contents present within the sediments i.e. hydrocarbon or water.

3.5 Petrophysical Analysis

Petrophysical analysis involves analyzing log data to calculate key reservoir properties such as net-to-gross, porosity, estimation of shale volume, permeability, water saturation, and hydrocarbon saturation. These properties are essential for characterizing the reservoir's ability to store and transmit fluids (Ebong et al., 2023a, b). Sand thicknesses was estimated with a view to determining the areas with good sand development, other petrophysical analysis carried out included estimation of sand/shale percentages, estimation of porosity, estimation of water and hydrocarbon saturation, delineation of possible hydrocarbon-bearing sands and also water, oil and gas contacts, estimation and comparison of porosity, permeability, water saturation, hydrocarbon saturation in and across the well(s) using the available wireline logs, estimation of shale volume content, bulk volume water, hydrocarbon pore volume/thicknesses, Net pay flag, cross plots of variable parameters, such as the different porosity logs.

3.5.1 Net-to-Gross Ratio (NTG)

Net thickness is often used alongside gross thickness to calculate the net-to-gross ratio (NTG), which represents the proportion of the gross interval that is productive. The Net-to-gross ratio was determined using the formula below:

$$NTG = \frac{Net\ thickness}{Gross\ thickness} \qquad (1)$$

3.5.2 Porosity

Porosity is the proportion of a given volume of rock that forms pore space and can thus hold liquid (Schlumberger, 1985). It is the fractional volume of pores in a rock, a relative quantity that is often expressed in decimal/fractional units or as a percentage. This volume of voids is useful for storing fluids like water, oil, and gas; if permeable, it may also transport these fluids to a lower-pressure zone. The porosity ϕ_T was estimated by inputting the bulk density measurements acquired from the density log within each reservoir into the following equation:

$$\phi_T = \frac{\rho_{mat} - \rho_{bulk}}{\rho_{mat} - \rho_{fluid}} \qquad (2)$$

where ρ_{mat} is density of sandstone, ρ_{bulk} is bulk density, ρ_{fluid} is fluid density. where density for sandstone is 2.65g/cm3 and fluid density is 1 g/cm3.

3.5.3 Estimate of Shale Volume

Shale volume (Vsh) is a critical parameter in reservoir characterization as it helps distinguish between clean reservoir rocks and shaly intervals. It is essential for determining the net pay, effective porosity, and overall reservoir quality. Shale volume was estimated using the gamma-ray (GR) log. The Gamma Ray Index (IGR) is given as:

$$IGR = \frac{GR_{\log} - GR_{\min}}{GR_{\max} - GR_{\min}} \qquad (3)$$

where IGR = Gamma ray index, $GR_{\log}$ = Gamma ray reading of the Formation, $GR_{\min}$ = Minimum gamma ray (clean sand) and $GR_{\max}$ = Maximum gamma ray (shale). Using Larionov (1969) equation for tertiary rocks, the shale volume is given by:

$$Vsh = 0.0083(2^{3.7 \times IGR} - 1) \qquad (4)$$

3.5.4 Water Saturation

Water saturation (Sw) is a crucial petrophysical parameter in reservoir characterization, representing the fraction of pore space in a rock

that is occupied by formation water. It is critical for determining hydrocarbon saturation (Sh), volumetric reserves, and production potential. Accurate estimation of Sw is essential for evaluating reservoir quality and planning hydrocarbon extraction. Water saturation is expressed as a percentage or fraction:

$$S_w = \frac{\text{Volume of Water in Pores}}{\text{Total Pore Volume}} \quad (5)$$

For this study, water saturation was calculated using the Archie's Equation below:

$$S_w^n = \frac{aR_w}{\phi^m R_t} \quad (6)$$

where S_w = water saturation, R_w = formation water resistivity, R_t = true formation resistivity, Φ = Porosity, a = Tortuosity factor (1), m = Cementation exponent (typically 1.8–2.0 for sandstones) and n = Saturation exponent (typically 2.0 for water-wet rocks).

3.6 Facies Identification

Facies identification is used to define and characterize different facies within the identified stratigraphic units, inferring their depositional environments and assessing their reservoir potential primarily from well log data. Given the absence of core data, the methodology mainly emphasized facies identification. This involves analyzing characteristic log responses, such as blocky, serrated, funnel, or bell-shaped Gamma Ray patterns, and their associated resistivity, density, and sonic values, to define distinct facies (Slatt, 2006). Based on the identified facies with their vertical and lateral relationships (from correlation panels), the prevailing depositional environments for each defined facies were interpreted by comparing observed facies assemblages with established depositional models (Walker, 1992). The absence of core data means that direct calibration will not be possible, increasing reliance on established log-facies relationships and regional geological analogues. The expected output includes defined facies, facies maps (if sufficient well control), and a depositional model for the reservoir units.

3.7 Sequence Stratigraphy

Sequence stratigraphy is to delineate the chronostratigraphic framework of the study area by identifying key sequence stratigraphic surfaces and systems tracts, thereby understanding the controls on sediment distribution and reservoir architecture following the principles laid out by Vail et al. (1977) and Van Wagoner et al. (1988). It involves the identification of sequence stratigraphic surfaces on both well logs and seismic data. On well logs, major sequence boundaries (SB), maximum flooding surfaces (MFS), and transgressive surfaces (TS) will be identified based on characteristic log motifs, abrupt changes in log patterns, shale content variations.

3.8 Seismic Interpretation

Seismic interpretation is a critical component of subsurface exploration and reservoir characterization, involving the analysis of seismic data to understand geological structures, stratigraphy, and rock properties in the subsurface (Ekanem et al., 2021). In contrast to the one-dimensional nature of a well bore, seismic data allows for a good portrayal of the earth's extremely complicated three-dimensional subsurface.

3.8.1 Synthetic Seismogram Generation

The sonic log, which is the reciprocal of velocity, was calibrated using check shot data. The calibration process is necessary to improve the quality of the sonic log because the sonic log is prone to washouts and other wellbore related issues. The results of calibrating the sonic log with the check shot gives the calibrated sonic log. The calibrated sonic log is used along with the density log to generate an acoustic impedance (AI) log. The acoustic impedance log is calculated for each layer of rock. The next step involves generating the reflectivity coefficient (RC) log. RC is calculated and generated using the AI log. The RC log

generated is then convolved with a wavelet to generate a synthetic seismogram which is comparable with the seismic data. The statistical wavelet utilized for convolution is extracted from seismic data. The synthetic seismogram was generated. The mathematical expressions that govern the entire well-to-seismic tie workflow are presented below:

$$AI = \rho v \quad (7)$$

$$RC = \frac{\rho_2 v_2 - \rho_1 v_1}{\rho_2 v_2 + \rho_1 v_1} \quad (8)$$

$$\text{Synthetic seismogram} = \frac{\rho_2 v_2 - \rho_1 v_1}{\rho_2 v_2 + \rho_1 v_1} * wavelet \quad (9)$$

where: AI = acoustic impedance, RC = reflection coefficient, ρ = density and v = velocity.

3.8.2 Seismic to Well Tie

A seismic-to-well tie is a crucial step in seismic interpretation that ensures the alignment of seismic data with subsurface geological features recorded in well logs. It establishes a robust relationship between time-based seismic data and depth-based well log data, enabling interpreters to correlate seismic reflectors with specific geological horizons. This process improves the accuracy of seismic interpretation and provides a direct link between seismic imaging and reservoir properties.

3.9 Fault Mapping

Faulted structures are important elements of the petroleum system as they play important roles in the trapping of hydrocarbon, making it imperative to ensure the use of correct and adequate techniques to map them. Faults in the seismic survey were identified based on criteria such as abrupt termination of reflection events; breaks in reflection events; abrupt lateral velocity changes; over-lapping of reflection events; pattern change of reflection events across a fault; structural deformation in beds above the fault zone; anomalous dip near the fault zone. The major faults in the seismic survey were identified and mapped along dip lines. To have a good resolution of the faults, a scroll increment of 10 lines was employed on both in-lines and cross-lines while picking the faults. Precautions were also made to ensure the consistency of the fault traces owing to the possibility that faults dying out can easily be mistaken for another in a field with a complex fault system. To ensure, a variance attribute was generated to amplify the discontinuities and guide the continual fault picking on subsequent lines.

3.9.1 Mapping of Horizons

Prior to the proper establishment of the stratigraphic framework of the field, identified stratigraphic horizons were mapped at every 5 msec on both inline and crossline across the seismic volume. The seeded horizon was used as input to generate the time surface maps for the horizons of interest.

3.9.2 Generation of Maps

Structural maps were generated from the mapped horizons that were picked on both cross line and inline to evaluate the geometry of the hydrocarbon zones. The horizon maps were generated in time, and the velocity model was used to produce a depth map to aid in the data interpretation.

3.10 Reservoir Geophysics

Seismic attributes will be extracted and analyzed for reservoir characterization, these include RMS (Root Mean Square) Amplitude to highlight high-amplitude zones indicative of potential hydrocarbon presence or thick sands; attributes like phase and frequency for continuity and discontinuity analysis, coherence/similarity to delineate faults, channels, and stratigraphic boundaries; and spectral decomposition to identify tuned intervals related to reservoir thickness and stratigraphy (Chopra & Marfurt, 2007). These attributes will enhance the visualization of reservoir geometry, delineate hydrocarbon accumulation zones, identify fluid contacts, and reveal internal reservoir heterogeneities.

3.11 Monte Carlo Simulation and Uncertainty Aggregation

Monte Carlo Simulation (MCS) enables a probabilistic assessment of hydrocarbon volumes by sampling input parameters according to their probability distributions and propagating uncertainties through the volumetric model (Udoinyang et al, 2019; Ekong et al., 2025). In this study, qualitative geological knowledge is combined with quantitative probabilistic methods to estimate the Expected Ultimate Recovery (EUR) and associated risks for the QX Field.

As an underlying assumption, input parameters are treated as independent when data indicate little or no correlation, which simplifies uncertainty analysis. For example, porosity and net pay from different depositional facies are considered independent. Where correlations exist, they can be incorporated using a correlation matrix or copula, for instance, the positive relationship between porosity and net pay in channel sands. Assuming independence allows the use of the Root Sum of Squares (RSS) method to combine uncertainties from multiple parameters. RSS provides a statistically sound and conservative estimate of overall uncertainty, remaining valid even when weak correlations are present, with a correlation coefficient < 0.3.

Input Parameter Identification

The volumetric hydrocarbon estimation formula for oil is typically given in Equation 10.

$$STOIIP/OOIP=7758\times A\times h\times \phi\times(1-Sw)\times Bo \quad (10)$$

where A = area (acre), h = net pay thickness (ft), ϕ = porosity (%), S_W = water saturation (%), and Bo = oil formation volume factor. Other parameters may include recovery factor (RF) for EUR, and gas-specific adjustments for GIP. Specifically, net pay determination was based on established cut-off criteria: volume of shale ($V_{sh} \leq 0.35$), effective porosity ($\phi \geq 0.10$), and water saturation ($S_w \leq 0.60$). Only intervals satisfying all three conditions were classified as hydrocarbon-bearing. Consequently, while some wells exhibit overall high Sw values when averaged across thick heterogeneous intervals, discrete sub-intervals within these reservoirs meet the hydrocarbon flagging criteria and constitute the actual pay zones. Volume estimation quantitatively estimates the Stock Tank Oil Initially in Place (STOIIP) or Gas Initially in Place (GIIP) for identifying hydrocarbon accumulations (Dake, 1978). This begins with a detailed petrophysical evaluation of well logs for the net reservoir intervals, calculating parameters such as shale volume (V-shale) derived from the Gamma Ray log, and porosity (ϕ) (Asquith & Krygowski, 2004). Water saturation (Sw) will be determined using appropriate petrophysical models, such as Archie's equation (Archie (1942), with input parameters like cementation exponent (m), saturation exponent (n), and tortuosity factor (a). The Net-to-Gross Ratio (N/G) will be calculated as the proportion of reservoir-quality rock (meeting defined porosity, shale, and water saturation cut-offs) within the gross reservoir interval. These petrophysical parameters were averaged for each reservoir zone from the available wells. The Gross Rock Volume (GRV) determination assisted in structurally interpreted depth maps of the top and base of the reservoir unit, combined with the fault derived from reservoir geophysics, to accurately calculate the (GRV) of the hydrocarbon accumulation within volume calculation module. Therefore, the hydrocarbon pore volume (HCPV) and the hydrocarbon volume were calculated using the following standard volumetric formula:

$$HCPV=A\times h\times N/G\times \phi\times(1-Sw) \quad (11)$$

where A = The Areal Extent, H = Gross Thickness (both from seismic interpretation and mapping), N/G= Net-To-Gross Ratio, ϕ = Average Effective Porosity, S_w = Average Water Saturation (all from petrophysical evaluation).

$$\text{Hydrocarbon Volume}_i = 7758\times A_i\times h_i\cdot\phi_i\times (1-Sw,_i)\times Bo_i\times RF_i \quad (12)$$

The Stock Tank Oil Initially in Place (STOIIP) was calculated as:

STOIIP = Hydrocarbon Pore Volume (HCPV)/Bo (13)

where Bo = Oil Formation Volume Factor. The Gas Initially in Place (GIIP) was calculated as:

$$GIIP = HCPV \times Fg \quad (14)$$

where Fg = Gas Expansion Factor, and Bo and Fg were obtained from regional analogues. Finally, Monte Carlo simulation, is recommended to assess the uncertainty in the volumetric estimates (Downey, 2005). This involves defining statistical distributions for key input parameters (A, h, N/G, ϕ, Sw, Bo/Fg) to generate P10 (optimistic), P50 (most likely), and P90 (pessimistic) hydrocarbon volume estimates.

To determine the final Total Field Volume, the P10, P50 and P90 values from the individual reservoir simulations must be aggregated probabilistically. Therefore, the Total Field P10 and P90 were calculated using the Variance Addition Method (Root Sum of Squares or RSS), assuming the individual reservoirs as being statistically independent (SPE, 2018)
The aggregation steps are:

Mean (P50): The P50 values are summed arithmetically.

$$P50Total = \sum P50i \quad (15)$$

Standard Deviation(σ): The standard deviation for each reservoir (Ri) is estimated from the P10-P90 range, and then the variances (σ^2) are summed:

$$\sigma_{Total} = \sqrt{\sum_{1}\left(\frac{P10_i - P90_i}{2.56}\right)^2} \quad (16)$$

Probabilistic range: the total P10 and P90 are calculated using the total mean and standard deviation:

$$P\,x\,Total = P50\,Total \pm 1.28 \times \sigma\,Total \quad (17)$$

The method correctly accounts for the portfolio effect, resulting in a statistically valid and narrower uncertainty range for the total field volume.

3.12 Well Log Correlation and Reservoir Delineation

A field wide correlation along strike from East to West using wells QX-02, QX-05, QX-01 and QX-04 was carried out by integrating gamma ray log, resistivity logs, density and Neutron porosity log. Tops and bases of three reservoirs (RES1, RES2 and RES3) were mapped using resistivity as a log-based hydrocarbon indicator (Figure 4). The occurrence and distribution of the lithostratigraphic units appear to reflect influence of basin morphology and sea level rise. There reservoirs are expressively continuous across all the wells in thickness and geometry. Sand thick fairly appears to decrease in some reservoirs in the east direction reflecting the character of deposition in the Niger Delta basin (Tuttle et al., 1999).

4.0 Result and Discussion

Field-wide correlation of the well logs (using a 60 API sand cut-off) clearly delineates three laterally continuous reservoir units (RES1–RES3), as illustrated in Figure 4. These reservoirs exhibit a systematic, though subtle, reduction in thickness toward the eastern part of the field. This lateral thinning trend is not arbitrary; rather, it reflects the progradational depositional architecture typical of the Niger Delta, where sediment supply, accommodation space, and shoreline migration collectively control reservoir geometry (Udo et al., 2020). The observed stratigraphic continuity across wells further suggests deposition within relatively stable and laterally extensive sedimentary environments, likely associated with deltaic channel–bar complexes and shoreface systems.

From an analytical standpoint, the consistency in reservoir stacking patterns across the field indicates a strong stratigraphic control on reservoir distribution. This reinforces the interpretation that the reservoirs are products of organized depositional processes rather than isolated or random sand bodies. The integration of well logs with seismic data and sequence

stratigraphic frameworks provides additional insight into the genetic relationships of these units, allowing for the identification of key stratigraphic surfaces such as flooding surfaces and sequence boundaries that govern reservoir compartmentalization and continuity (Xu et al., 2025).

Reservoir quality across RES1–RES3 is generally favorable, as evidenced by log responses indicative of clean, well-sorted sands. However, subtle heterogeneities are observed within and between the reservoir units, likely arising from variations in depositional energy, grain size distribution, and post-depositional diagenetic processes. These heterogeneities have important implications for fluid flow behavior, connectivity, and ultimate recovery.

A key outcome of the integrated analysis is the improved discrimination of fluid types within the reservoirs. Specifically, RES2 is interpreted to be predominantly gas-bearing, while RES1 and RES3 are characterized by oil accumulations. This differentiation is supported by combined petrophysical signatures and seismic attributes, which enhance confidence in fluid prediction compared to single-dataset interpretations. Consequently, the integration of multidisciplinary datasets not only reduces subsurface uncertainty but also provides a more robust basis for reservoir modeling, volumetric estimation, and field development planning.

In all, the results demonstrate that a holistic, data-integrated approach significantly enhances the reliability of reservoir characterization, enabling more informed and economically sound development decisions.

4.1 Sequence Stratigraphy/ Facies Identification

Analysis of the well log motifs (Figure 5) indicates the presence of two third-order depositional sequences, extending from RES3 at the base to RES1 at the top. These sequences reflect changing depositional conditions driven by relative sea-level fluctuations and sediment supply. A clear upward trend is observed in reservoir development. RES3 is thinner and more shale-prone, while RES2 and RES1 show increased sand thickness and better reservoir continuity. This vertical evolution suggests an initial marine-dominated transgressive phase, followed by improved sand deposition as conditions became more favorable for sediment accumulation. Facies distribution supports this interpretation. RES1 and RES2 contain channel sands, upper shoreface sands, and shales, indicating a mix of fluvial input and marine reworking. In contrast, RES3 is dominated by shoreface and shale facies, reflecting a more marine setting with limited channel influence.

These depositional differences directly control reservoir quality. Shoreface sands provide the most laterally continuous and reliable reservoir units, supporting better connectivity and fluid flow. Channel sands, although cleaner and potentially high in porosity and permeability, are less continuous, which may lead to compartmentalization. Meanwhile, shale intervals act as barriers, reducing vertical communication between reservoir layers (Udoinyang et al., 2019).

In terms of fluid distribution, the more continuous shoreface sands favor stable and predictable hydrocarbon accumulation, whereas channelized units may host localized or discontinuous fluid pockets. This heterogeneity is critical, as it influences sweep efficiency and recovery. The reservoir quality improves upward from RES3 to RES1, with increasing sand dominance and connectivity. This vertical variation is key to understanding net-to-gross distribution, flow behavior, and uncertainty in volumetric estimates, particularly when integrated into probabilistic models such as Monte Carlo simulation. Generally, the sedimentary setting is predominantly deltaic and comprises fluvial/distributary channels and shoreface. Res 1 and 2 however, were deposited in channelized shoreface setting while Res 3 was deposited in a lower shoreface environment. The well log correlation panel integrating wells QX 02, QX 05, QX 01, and QX

04 in Figure 6 forms the foundation for the sequence stratigraphic interpretation and provides a coherent framework for understanding depositional processes and reservoir distribution across the field.

The well log correlation panel integrating wells QX 02, QX 05, QX 01, and QX 04 in Figure 6 forms the foundation for the sequence stratigraphic interpretation and provides a coherent framework for understanding depositional processes and reservoir distribution across the field. The analysis draws primarily on Gamma Ray and resistivity log responses, which together offer reliable indicators of lithology and fluid content. Through careful correlation of these logs, stratigraphic continuity and variations in facies architecture are clearly established. The depositional setting is interpreted as a wave and river influenced deltaic system shaped by repeated fluctuations in relative sea level. These fluctuations, driven by a combination of eustatic changes and tectonic influences, controlled the balance between sediment supply and accommodation space. As a result, the stratigraphic record preserves a cyclic pattern of shoreline advance, vertical build up, and occasional landward retreat. This dynamic interplay is reflected in the stacking patterns observed across the wells and explains the lateral persistence of key reservoir units.

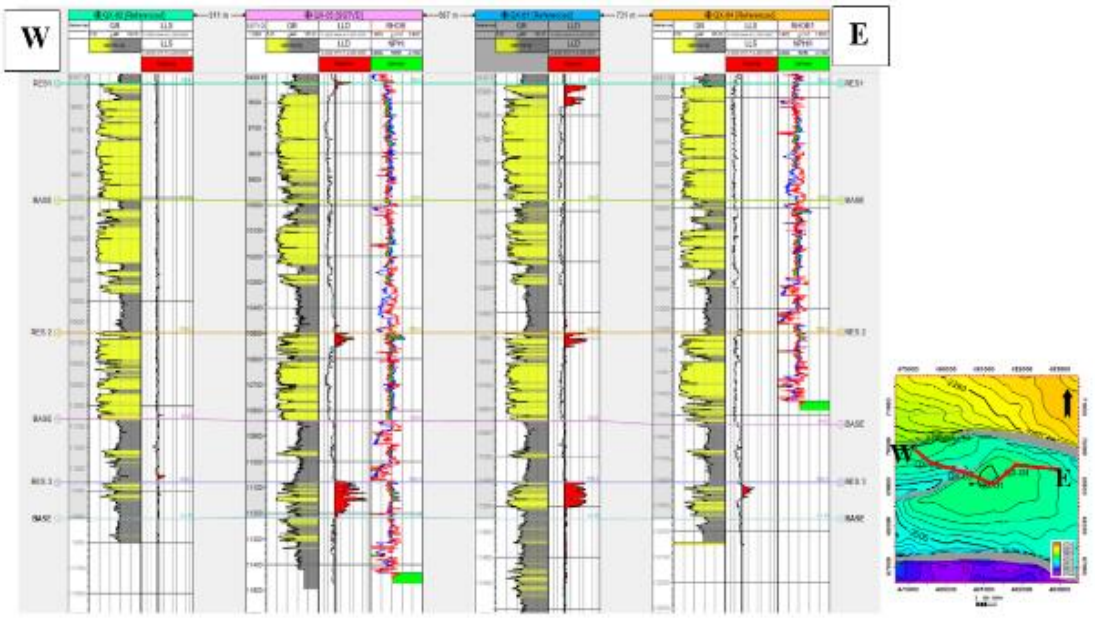

Figure 4.: Well log Correlation (sand cut-off: 60API)

Key stratigraphic surfaces provide important markers for subdividing the succession into genetically related units. Sequence boundaries identified as SB 1 and SB 2 appear as sharp breaks on the Gamma Ray logs and indicate periods of relative sea level fall. These surfaces are associated with subaerial exposure or basin-ward erosion and mark the onset of new depositional cycles. In contrast, maximum flooding surfaces labeled MFS 1, MFS 2, and MFS 3 represent intervals of maximum marine influence. They are expressed as pronounced Gamma Ray peaks, reflecting the accumulation of fine-grained marine sediments under the deepest water conditions within each cycle. Between these bounding surfaces, the succession is organized into distinct systems tracts that record the evolution of depositional environments through time. The Lowstand Systems Tract occurs immediately above the sequence boundaries and is particularly well developed in wells QX 01 and QX 04. Here, the logs display blocky Gamma Ray signatures that correspond to thick, clean sand bodies interpreted as channel deposits. These features indicate high energy conditions and rapid

sediment transport across an exposed shelf, suggesting efficient sediment delivery into the basin during periods of lowered sea level (Ma et al., 2025). Above this, the Transgressive Systems Tract reflects a progressive rise in sea level and a corresponding landward shift of depositional environments. This interval is characterized by a consistent increase in Gamma Ray values, indicating a transition from coarser to finer sediments. The overall fining upward trend captures the gradual encroachment of marine conditions and reduced energy levels as accommodation space increases faster than sediment supply.

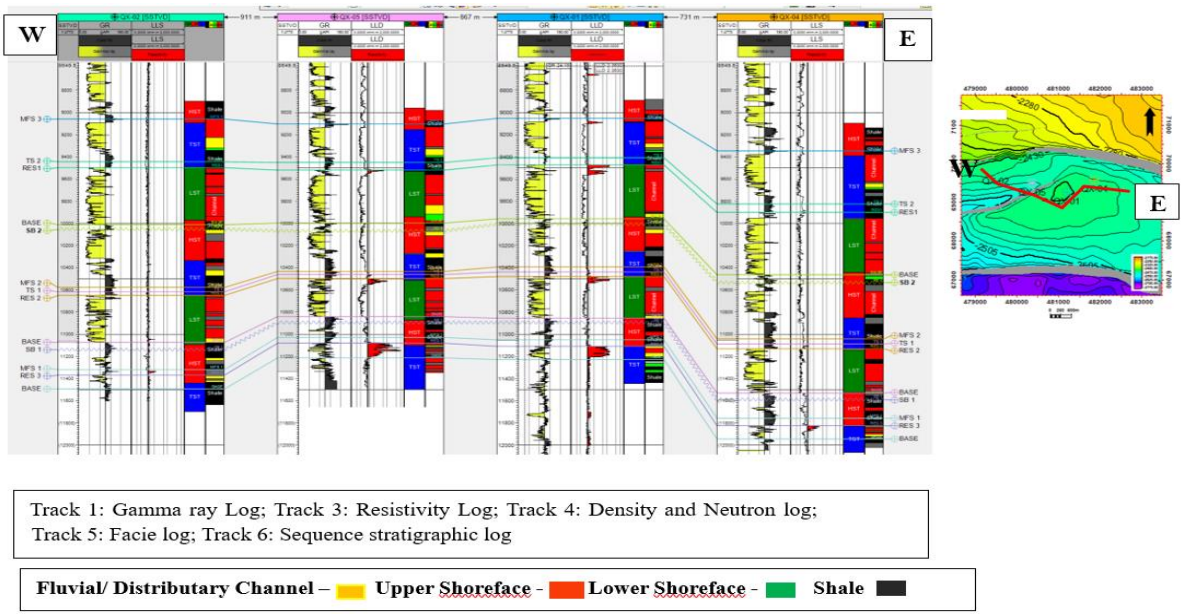

Fig. 5: Facie/Sequences stratigraphic framework of QX – field

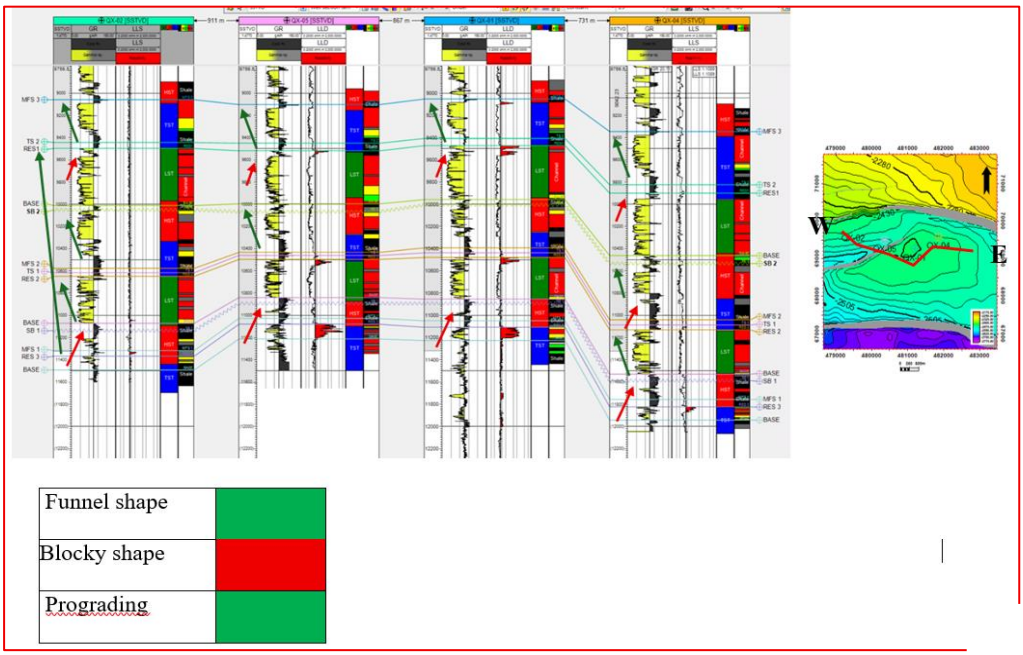

Figure 6: Well log signatures to determine the sequence stratigraphy of QX – field

The Highstand Systems Tract overlies the maximum flooding surfaces and records a return to more active sedimentation as supply begins to exceed accommodation. This phase is marked by a coarsening upward trend on the logs, indicating renewed progradation and the outward growth of the delta front. The stacking pattern suggests a gradual seaward advance of

facies, preparing the system for the next cycle of relative sea level fall.

Resistivity responses provide further insight into reservoir quality and fluid distribution. Intervals such as RES1 and other sands within the lowstand and highstand deposits show consistently high resistivity values, supporting the presence of hydrocarbon charged reservoirs. The association of these reservoirs with both lowstand channel sands and highstand prograding units highlights the importance of depositional energy and stratigraphic position in controlling reservoir development.

Overall, the integration of log signatures with sequence stratigraphic concepts reveals a highly organized depositional system in which reservoir distribution is far from random. Instead, it is strongly governed by the interaction between sea level changes, sediment supply, and basin dynamics. This understanding not only enhances confidence in reservoir prediction but also provides a robust framework for identifying prospective zones within the field.

4.2 Petrophysical Evaluation

Tables 3 and 4 present a comprehensive summary of the standard facies-based petrophysical classifications and the quantitative reservoir evaluation for the QX Field. The analysis focuses on key reservoir quality indicators, including Net-to-Gross (NTG), effective porosity (PHIE), volume of shale (VSH), water saturation (Sw), and permeability (K), which collectively define reservoir performance and hydrocarbon potential.

The results indicate that NTG values range from 60% to 87%, reflecting a generally high proportion of clean, reservoir-quality sands relative to non-reservoir intervals. This suggests good reservoir continuity and favorable depositional conditions, likely associated with channelized or shoreface sand bodies typical of paralic settings. Effective porosity values between 18% and 25% further support this interpretation, indicating moderate to good pore connectivity and storage capacity. These porosity values fall within the expected range for productive reservoirs and imply limited compaction or cementation effects, especially in the shallower intervals. The volume of shale (VSH), which varies from 13% to 40%, reveals moderate heterogeneity within the reservoir units. Lower VSH intervals correspond to cleaner sands with better reservoir quality, while higher shale content suggests interbedding or lamination that may reduce permeability and fluid flow efficiency. This heterogeneity is consistent with depositional environments characterized by fluctuating energy conditions, such as deltaic or distributary channel systems.

Water saturation (Sw) exhibits a wide range from 20% to 99%, indicating significant variation in fluid distribution across the reservoirs. Intervals with lower Sw values are indicative of hydrocarbon-bearing zones, whereas higher values suggest water-dominated or residual hydrocarbon zones. This variability highlights the importance of integrating petrophysical interpretation with structural and stratigraphic controls to accurately delineate hydrocarbon-bearing intervals.

Permeability values ranging from 37.28 mD to 219.73 mD suggest fair to very good reservoir transmissibility. Higher permeability zones are likely associated with well-sorted, coarse-grained sands, while lower values may reflect the influence of shale content or diagenetic effects. Overall, the permeability distribution supports the potential for efficient fluid flow in the better-quality reservoir intervals. Based on these parameters, the reservoirs can be classified as having fair to good quality, consistent with the qualitative assessment presented in Table 4. The observed petrophysical properties are also comparable to established values reported for reservoirs within the Niger Delta, reinforcing the reliability of the interpretation and the regional geological consistency. A notable trend observed in the data

is the systematic reduction in reservoir quality with increasing depth and thickness. This decline is likely attributable to compaction, increased overburden pressure, and diagenetic processes such as cementation, which reduce pore space and connectivity. Additionally, thicker reservoir units may incorporate more heterolithic facies, contributing to increased shale content and reduced overall quality.

Overall, the integrated petrophysical evaluation demonstrates that reservoir quality in the QX Field is primarily controlled by depositional environment and post-depositional modifications, with clear implications for reservoir distribution, heterogeneity, and hydrocarbon productivity.

Table 3: Combined porosity and permeability classification chart (Etu-Efeotor, 1997)

Reservoir quality	Porosity (%)	Permeability (mD)
Excellent	>25	>1000
Good	20 – 25	100 -1000
Fair	15 – 20	10 – 100
Poor	10 -15	1 – 10
Very poor	< 10	< 1

Table 4: Result of the Petrophysical Evaluation

WELLS	RESERVOIR	GROSS (ft)	NET (ft)	NTG (%)	PHIE (%)	VSH (%)	Sw (%)	K (mD)
QX-01	RES 1	479	402.36	84	23	16	12	140.07
	RES 2	378	291.06	77	24	23	17	176.26
	RES 3	105	77.7	74	20	26	29	65.85
QX-02	RES 1	508.5	417.06	82	23	18	100	140.07
	RES 2	410	328	80	22	20	100	110.18
	RES 3	62	42.16	68	18	32	98	37.28
QX-04	RES 1	507	441.09	87	22	13	98	110.18
	RES2	399	303.24	76	24	24	99	176.26
	RES3	121	72.6	60	19	40	82	49.92
QX-05	RES 1	392	337.12	86	25	14	80	219.73
	RES 2	338	280.54	83	23	17	78	140.07
	RES 3	81	60.75	75	21	25	22	85.70

4.3 Petrophysical Characteristics of Reservoir 1

Based on Table 3, Reservoir 1 (RES1) exhibits consistently high reservoir quality across all wells, as reflected in its thickness, porosity, and permeability distributions. The gross thickness ranges from 392 ft to 508.5 ft, with an average of 471.63 ft, while the net thickness varies between 337.12 ft and 441.09 ft, averaging 399.41 ft (Figure 7). This relatively high net thickness indicates substantial reservoir development and continuity across the field.

The Net-to-Gross (NTG) ratio ranges from 82% to 87%, with an average value of 84.75% (Figure 7), suggesting a dominantly sandy lithology with minimal non-reservoir intercalations. This high NTG reflects favorable depositional conditions, likely associated with high-energy environments that promoted clean sand accumulation. The effective

porosity (PHIE) values range between 22% and 25%, with an average of 23.25%, indicating excellent pore space for hydrocarbon storage. In conjunction with evaluated properties, the volume of shale (VSH) varies from 13% to 18% (average 15.25%), confirming relatively low shale content and minimal pore space obstruction (Figure 8). This further supports the interpretation of a clean and well-sorted reservoir unit.

However, the water saturation (S_w) values require careful interpretation. The reported range (~12% to 100% or 88% to 100%) suggests significant variability and possible inconsistencies in estimation. If the lower bound is ~12%, it indicates hydrocarbon-bearing zones with good saturation; conversely, values approaching 100% imply water-bearing intervals or transition zones. The relatively high average Sw of 82.50% suggests that a significant portion of the reservoir may be water-saturated, which could reduce hydrocarbon productivity unless localized low-Sw zones are targeted (Figure 8).

The permeability (K) ranges from 140.07 mD to 219.73 mD, with an average of 152.51 mD, indicating good to very good fluid flow capacity. This level of permeability supports efficient fluid transmissivity and enhances the reservoir's producibility (Figure 9).

In all, the integration of high porosity and moderate-to-high permeability suggests that RES1 possesses good reservoir quality, with strong storage capacity and favorable flow characteristics. Nevertheless, the high-water saturation values may pose challenges to hydrocarbon recovery, emphasizing the need for careful reservoir zonation and fluid discrimination.

4.4 Petrophysical Characteristics of Reservoir 2

Reservoir 2 (RES2) also demonstrates favorable petrophysical properties, although with slightly lower quality compared to RES1 (Figure 7). The gross thickness ranges from 338 ft to 410 ft, with an average of 381.25 ft, while the net thickness varies from 280.54 ft to 328 ft, averaging 300.71 ft. These values indicate a moderately thick and laterally persistent reservoir unit. The Net-to-Gross ratio ranges from 76% to 83%, with an average of 79%, which is slightly lower than that of RES1. This suggests increased heterogeneity and a higher proportion of non-reservoir materials, likely reflecting more variable depositional conditions.

The effective porosity ranges from 22% to 24%, with an average of 23.25%, comparable to RES1 and indicative of good storage capacity (Figure 8). However, the volume of shale is relatively higher, ranging from 17% to 24% (average 21%), implying greater shale influence. This may reduce effective pore connectivity and slightly impair fluid flow. The water saturation (Sw) ranges from 83% to 100%, with an average of 93.00%, indicating that RES2 is predominantly water-bearing. Such high saturation values significantly limit hydrocarbon potential and suggest that the reservoir may either be located below the hydrocarbon-water contact or represent a transition zone (Meng et al., 2023).

Despite this, the permeability ranges from 110.18 mD to 176.26 mD, with an average of 150.69 mD, which still falls within the good range for fluid flow (Figure 9). This indicates that, where hydrocarbons are present, the reservoir could support efficient production.

Earnestly, RES2 exhibits moderate to good reservoir quality, characterized by adequate porosity and permeability but relatively higher shale content and significantly elevated water saturation. While its storage and transmissivity properties are favorable, the high-water saturation suggests limited hydrocarbon prospectivity compared to RES1, making fluid typing and saturation modeling critical for optimal reservoir evaluation.

4.5 Petrophysical Characteristics of Reservoir 3

The petrophysical evaluation of RES 3 reveals moderate reservoir development with noticeable heterogeneity across the interval. Gross thickness varies from 62 ft to 121 ft, while net thickness ranges between 42.16 ft and 77.7 ft,

with average values of 92.25 ft and 63.3 ft, respectively (Figure 7). This indicates that a significant proportion of the gross interval contributes to hydrocarbon storage, although some portions are affected by non-reservoir facies or shale intercalations.

The Net-to-Gross (NTG) ratio, ranging from 68% to 74% (average ≈ 79%), suggests relatively good reservoir continuity and sand development. Such NTG values are indicative of a dominantly sandy depositional system, likely with intermittent shale streaks that may introduce vertical heterogeneity and minor flow barriers. This is further supported by the Volume of Shale (Vsh), which ranges from 25% to 40% (average 30.75%), implying moderate shale content that could adversely affect both porosity and permeability through pore throat reduction and clay-related effects.

Effective porosity (Φe) values between 18% and 21% (average 19.50%) indicate fair storage capacity (Figure 8). While these values fall within acceptable ranges for productive reservoirs, they are not sufficiently high to be classified as excellent, suggesting that pore connectivity and storage efficiency may be somewhat limited. This observation is consistent with the moderate shale volume, which likely contributes to reduced pore space efficiency.

Water saturation (Sw) exhibits a very wide range from 22% to 98% (average 57.75%), highlighting significant fluid variability within the reservoir. The lower bound suggests the presence of hydrocarbon-bearing zones, whereas the extremely high upper values point to intervals that are predominantly water-bearing. This variability may reflect reservoir compartmentalization, differences in structural positioning (e.g., proximity to the water contact), or variations in reservoir quality and pore structure. Permeability values range from 37.28 mD to 85.70 mD, with an average of 59.68 mD, indicating fair to moderate fluid flow capacity (Figure 9). Although these values suggest that the reservoir is capable of transmitting fluids, they are not sufficiently high to ensure optimal production rates without assistance. The moderate permeability is likely influenced by the combined effects of shale content and pore throat geometry.

Overall, RES 3 can be classified as a fair-quality reservoir with moderate storage capacity and fair deliverability. The interplay of moderate porosity, permeability, and relatively high shale volume suggests that production performance may be constrained by formation heterogeneity and fluid distribution. Consequently, while the reservoir is potentially productive, optimal hydrocarbon recovery may require stimulation techniques such as hydraulic fracturing or acidizing to enhance permeability and improve flow efficiency.

4.5 Comparative Analysis

The petrophysical evaluation of the QX Field reservoirs indicates marked variations in reservoir quality across the three main intervals (RES1, RES2, and RES3). RES1 and RES2 consistently demonstrate superior reservoir characteristics relative to the deeper RES3, reflecting both depositional controls and diagenetic influences. As illustrated in Figure 7, RES1 and RES2 possess higher gross and net thicknesses, suggesting more substantial hydrocarbon-bearing intervals and enhanced storage potential. This thickness advantage is further reinforced by the Net-to-Gross (NTG) ratios (Figure 8), where RES1 and RES2 display significantly higher values compared to RES3. This pattern indicates more laterally continuous, cleaner sand bodies in the shallower reservoirs, which are likely to facilitate better connectivity and flow pathways for hydrocarbons. Porosity trends corroborate these observations. RES1 and RES2 exhibit elevated effective porosity, suggesting enhanced pore storage and potential hydrocarbon saturation. In contrast, RES3, despite its greater depth, shows comparatively lower porosity, indicating reduced storage capacity.

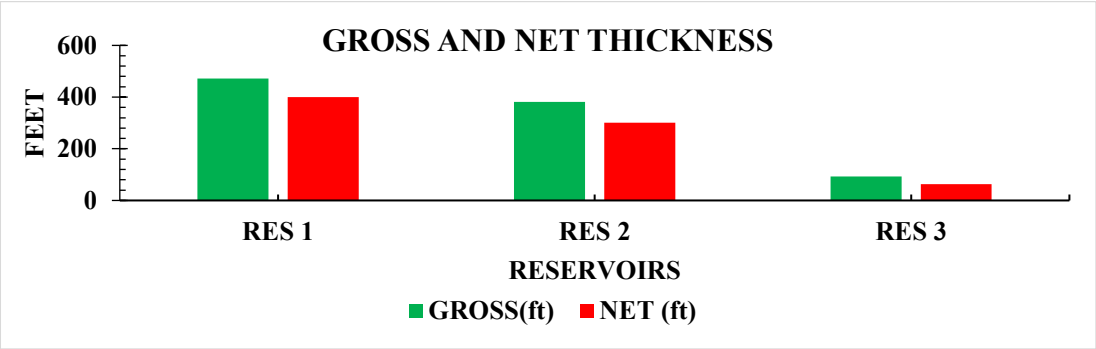

Figure 7: Histogram plot of average reservoir Gross and Net thickness

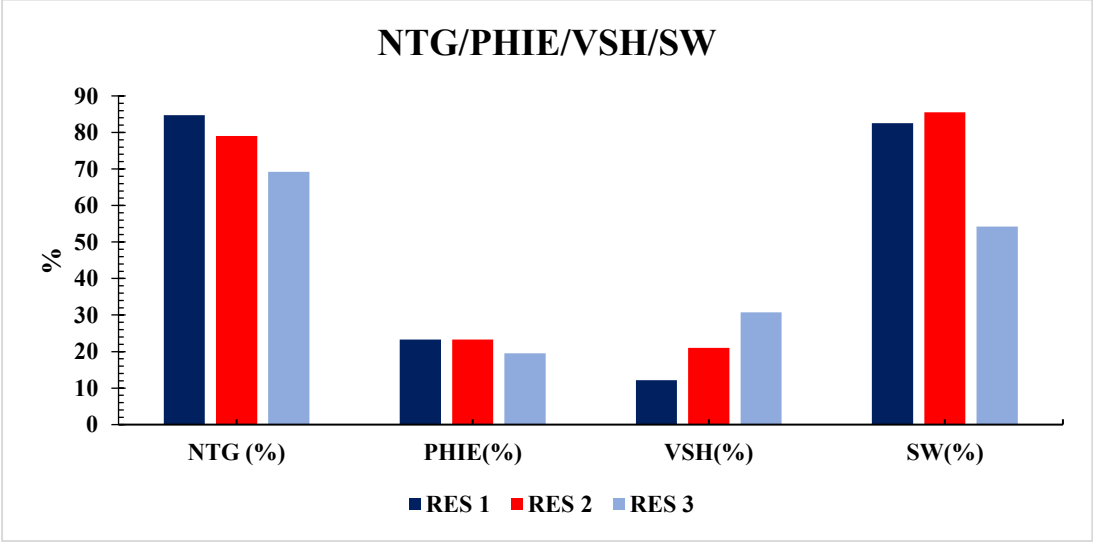

Figure 8: Histogram plot of average reservoir Net-to-Gross, Effective porosity, Volume of Shale and Water saturation

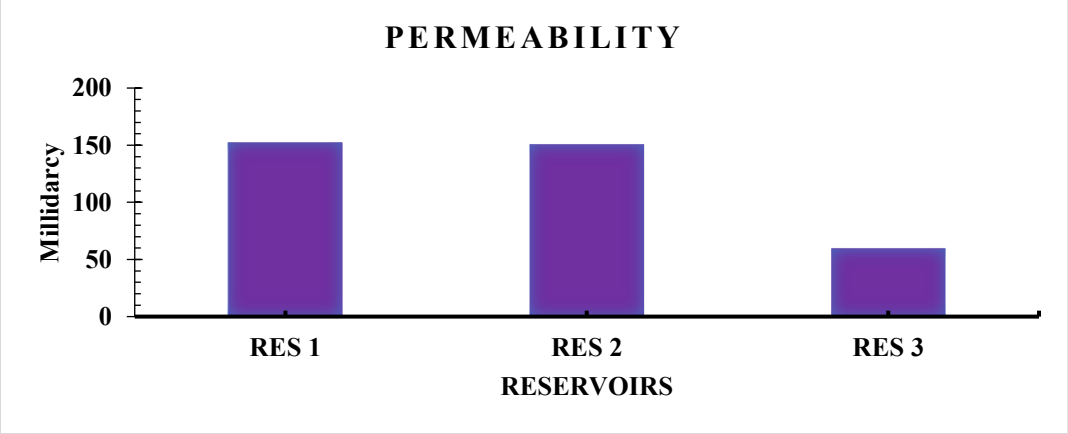

Figure 9: Histogram plot of average reservoir Permeability

Interestingly, shale volume (VSH) presents an inverse trend: RES3 has the lowest VSH, suggesting relatively pure sand content, whereas RES1 and RES2 show higher shale proportions. This heterogeneity may impact fluid distribution, creating pockets of variable saturation that could influence production efficiency.

Water saturation analysis reveals that RES1 and RES2 maintain relatively higher average water saturations than RES3. However, it is important to note that these values represent averages across both fully and partially saturated zones (García-Gutiérrez et al., 2023). Localized deviations likely exist, with some wells in RES1 and RES2 potentially displaying higher

hydrocarbon saturations (and correspondingly lower water saturations), highlighting the presence of compartmentalization or facies-controlled heterogeneity. Permeability data supports these interpretations: RES1 and RES2 exhibit superior fluid flow potential compared to RES3, consistent with their thicker, cleaner, and more porous intervals. Collectively, these results suggest that RES1 and RES2 represent the most prospective reservoirs in the QX Field in terms of hydrocarbon storage and producibility, whereas RES3, although showing some favorable attributes such as low VSH, is comparatively less promising. The contrast in petrophysical properties between the shallower and deeper reservoirs underscores the influence of depositional environment, burial history, and diagenetic alteration on reservoir quality.

4.6 Reservoir Mapping

Reservoir mapping of RES1, RES2, and RES3 was achieved by integrating well log data with seismic interpretations using available check-shot information. Synthetic seismograms were generated to ensure that reservoir tops are accurately tied to corresponding seismic reflections (Figure 10), providing a reliable framework for time–depth conversion and structural correlation (Akpan et al., 2020a).

Within the time interval of approximately 2200–3000 ms, all three reservoirs were mapped (Figure 11) and interpreted as structural prospects with 3-way fault closures. Hydrocarbon typing from Density and Neutron porosity logs suggests that RES1, RES2, and RES3 are most likely gas/oil, gas, and oil-bearing, respectively. Detailed contacts and pay thicknesses were interpreted as follows: RES1 exhibits a Gas-Oil Contact (GOC) at –9496 ftss and an Oil-Water Contact (OWC) at –9533 ftss, with predicted gas and oil pay thicknesses of 22.15 ft (6.75 m) and 37 ft (11.28 m), respectively (Table 5). RES2 has a Gas-Water Contact (GWC) at –10523 ftss with a predicted gas pay thickness of 28 ft (8.5 m), whereas RES3 shows an Oil-Water Contact (OWC) at –11200 ftss and an oil pay thickness of approximately 92.53 ft (28.3 m).

The interpreted seismic sections reveal a moderately dipping stratigraphic succession characterized by laterally continuous reflections (Akpan et al., 2020b). A prominent listric fault constitutes the dominant structural feature, producing significant reflector offsets and fault-bounded compartments. Adjacent to the fault, thickness variations indicate syn-depositional activity that influenced sediment accumulation, creating localized depocentres. These depocentres coincide with slightly thicker reservoir intervals, potentially enhancing hydrocarbon storage. Reservoir horizons tied to well data demonstrate strong, continuous seismic responses, allowing confident lateral correlation across the study area. Structural mapping confirms well-defined closures along the updip sections, which correspond to the placement of exploration wells, providing clear targets for hydrocarbon accumulation.

Moreover, the integration of well logs and seismic data enables a detailed understanding of both reservoir architecture and structural controls, highlighting the combined effects of deposition, faulting, and stratigraphic continuity on hydrocarbon distribution and recoverable volumes in the QX Field.

Furthermore, the spatial distribution of the reservoirs was systematically mapped across the seismic dataset, enabling the generation of reservoir representative time maps (Figures 12–14). These maps provide a detailed visualization of lateral and vertical variations within each reservoir, highlighting trends in thickness, continuity, and potential heterogeneity (Akpan et al., 2022a). Such representations are essential for subsequent analyses, including reservoir connectivity assessment, flow simulation, and identification of high-quality hydrocarbon-bearing zones, thereby enhancing the predictive understanding of reservoir behavior across the study area.

Table 5: Contact information and Predicted gas and oil pay thickness

Reservoir	GOC (ftss)	OWC (ftss)	GWC (ftss)	PGT (ft)	OPT (ft)
RES 1	9496	9533	-	22.15	37
RES 2	-	-	10523	28	-
RES 3	-	11200	-	-	28.30

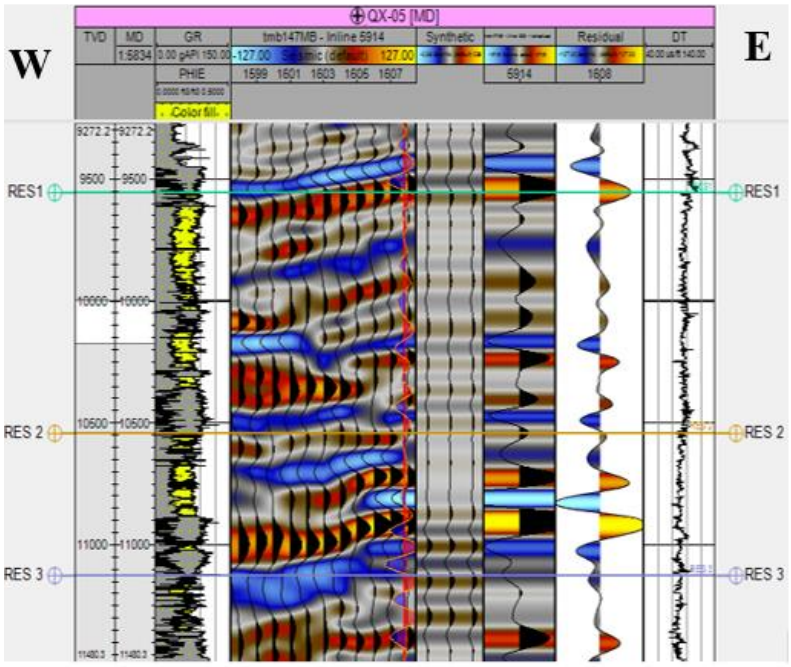

Figure 10: Synthetic seismogram along well QX-5 in the study area

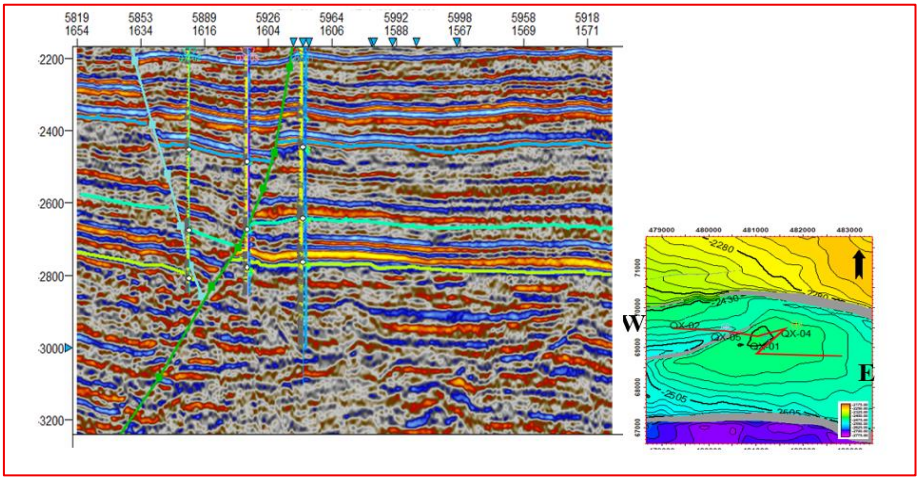

Figure 11: Arbitrary Seismic section along all the wells showing all the Reservoirs mapped

4.7 Reservoir Geophysics

Root Mean Square (RMS) amplitude was utilized to ascertain pore filled and fluid contact most of. The result from the attribute analysis was used to calibrate petrophysical log evaluation especially porosity to check for consistency. The windows used for this extraction was restricted to the time window that corresponds to the reservoir's gross thickness. Hence, the RMS amplitude extraction was carried out for all the reservoirs based on the polarity type at the top of the reservoir. On this note, RES1, RES 2 and RES 3 utilized peak, trough and zero crossing -/+ polarities, respectively.

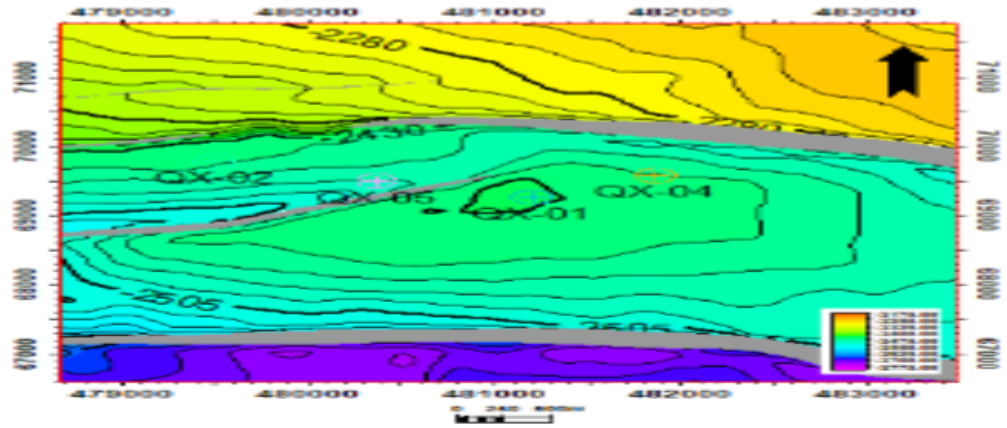

Figure 12: Time structural Map for RES 1

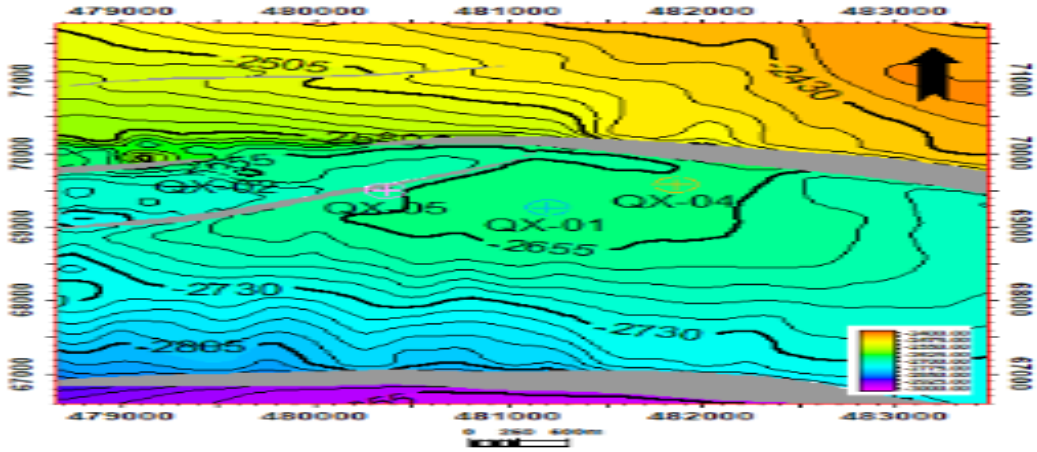

Figure 13: Time structural Map for RES2

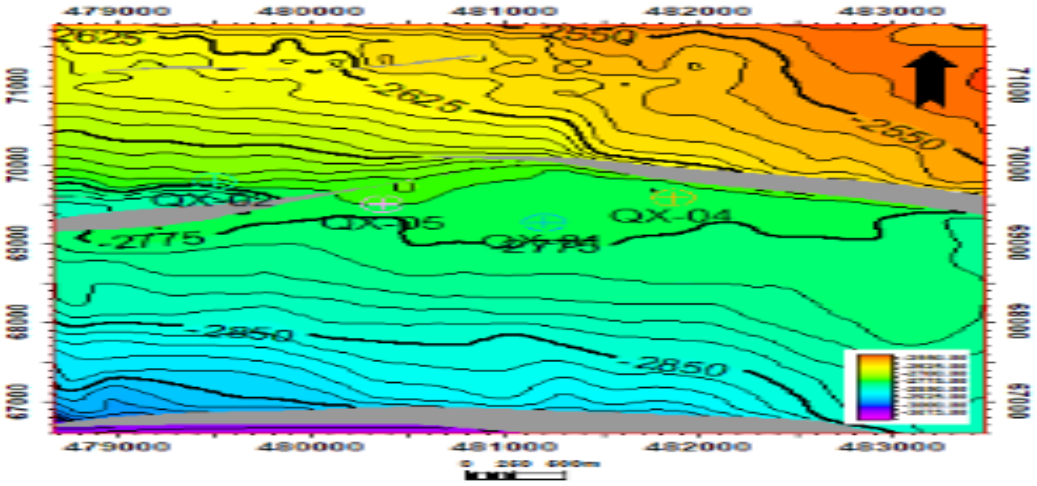

Figure 14: Time structural Map for RES3

Based on the amplitude map in Figures 15-17, Res 1 (Figure 15) is characterized by clearly defined amplitude shutoff across the hydrocarbon water interface as amplitude conforms excellently to structure. It also further affirms the likelihood of the good porosity and permeability gotten from the petrophysical evaluation. RES 2 (Figure 16) on the other hand showed a dull and patchy amplitude with no clear amplitude shutoff to define hydrocarbon water contact. In this situation amplitude was slightly not consistent with the petrophysical result but it would be reliable most likely. Based on the amplitude map also, RES 3 (Figure 17) showed conformance to structure and a strong

hydrocarbon-brine shutoff notwithstanding the fair petrophysical result from well location other reservoir location showed good reservoir quality based on the amplitude map although amplitude observably dull in some part.

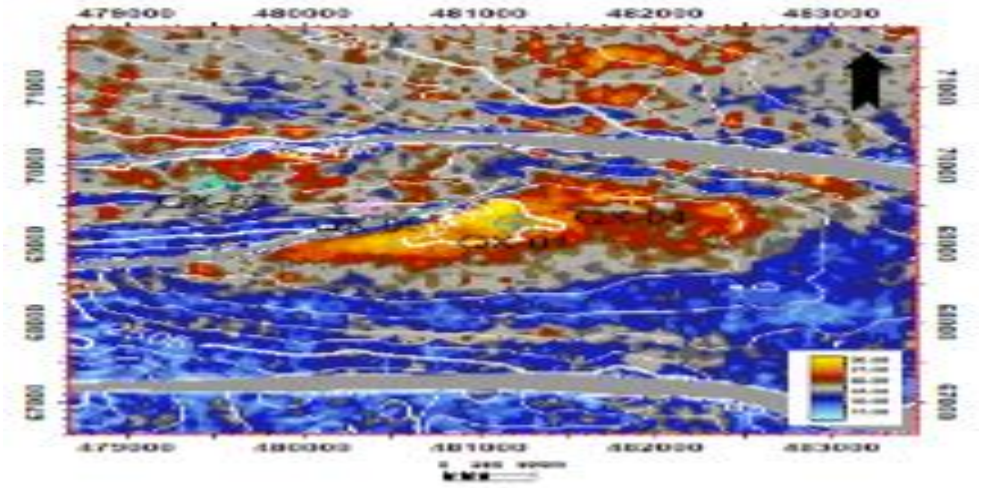

Figure 15: RMS amplitude maps for RES 1

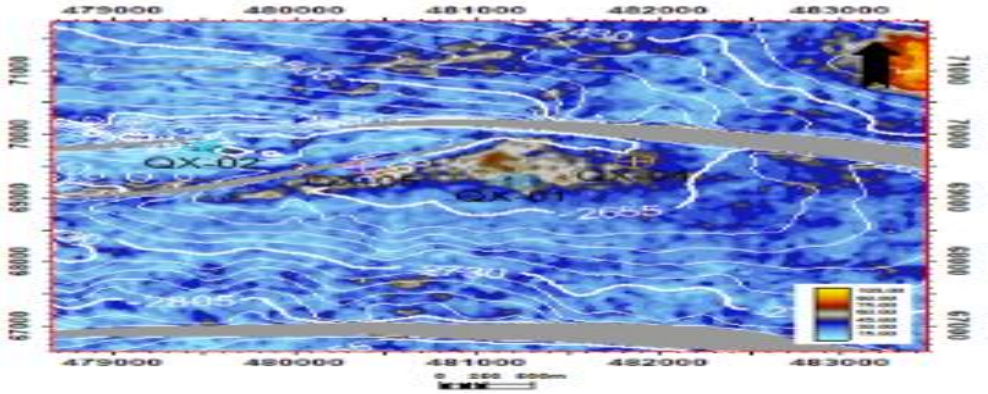

Figure 16: RMS amplitude maps for RES 2

4.8 Volumetric Estimation

The time structural maps were converted into depth structural maps using the simple velocity model outlined in the methodology, enabling accurate spatial representation of reservoir geometries. The high-case hydrocarbon contact information was superimposed on the depth maps, as illustrated in Figures 18–20, facilitating delineation of the hydrocarbon-bearing areas. For RES 1 (Figure 18), the oil-bearing interval was estimated to cover approximately 427.33 acres, while the gas-bearing interval extended over 601.23 acres. RES 2 (Figure 19) exhibited a gas-bearing area of 459.04 acres, highlighting a significant lateral continuity of the gas column. In RES 3 (Figure 20), the oil-bearing interval was more extensive, covering 776.39 acres, suggesting that RES 3, despite being deeper, contains a larger areal extent of hydrocarbons compared to RES 1.

Integrating these areal extents with the petrophysical parameters derived from well log analyses allowed for the computation of volumetric estimates of hydrocarbons (Ekong et al., 2025). The Stock Tank Oil Initially in Place (STOIIP) and Gas Initially in Place (GIIP) for each reservoir were calculated and summarized in Table 6. Additionally, a Monte Carlo simulation was performed to quantify uncertainty in these estimates, providing a probabilistic assessment across three scenarios: high-case (P10), most-likely (P50), and low-case (P90).

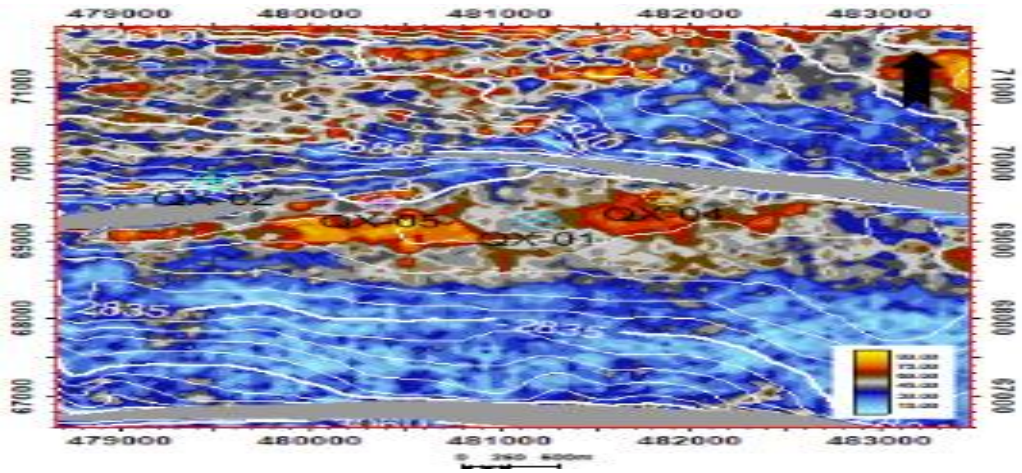

Figure 17: RMS amplitude maps for RES 3

A key observation from the volumetric analysis is that RES 1, despite having significant hydrocarbon presence, shows a lower STOIIP compared to RES 3. This outcome can be attributed to the combined effect of higher water saturation and thinner net oil pay within RES 1, limiting its effective hydrocarbon storage capacity. Conversely, RES 3 benefits from a thicker oil interval and lower water saturation, translating to higher volumetric potential.

At the field level, the probabilistic assessment indicates that the total QX Field holds a most-likely (P50) oil volume of 64.40 MMSTB and a corresponding gas volume of 12.20 BCF, reflecting substantial hydrocarbon potential. The results emphasize the importance of integrating areal mapping with petrophysical evaluation to obtain realistic and geologically consistent volumetric estimates.

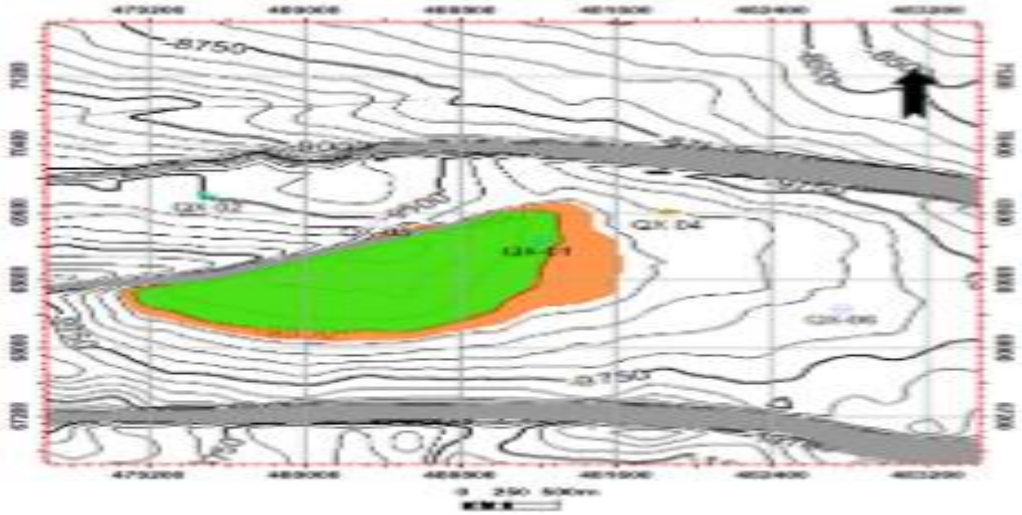

Figure 18: Depth structural maps for RES 1

The final stage of the volumetric assessment involved aggregating the individual reservoir results to derive the Total Field Volume, providing a comprehensive picture of the hydrocarbon potential across the QX Field. As illustrated in Figure 21, this step underscores the necessity of a probabilistic approach rather than relying solely on deterministic arithmetic calculations. A direct comparison between the Arithmetic Sum (simply adding the P10, P50, and P90 estimates of each reservoir) and the Probabilistic Total (obtained using the Variance Addition Method, or Root-Sum-of-Squares, RSS) highlights the effect of combining independent reservoirs, known as the Portfolio Effect.

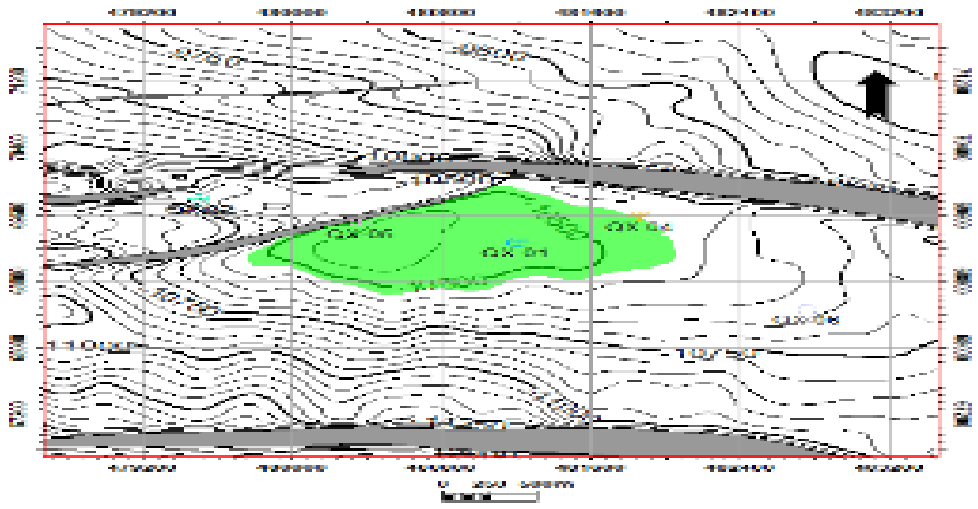

Figure 19: Depth structural maps for RES 2

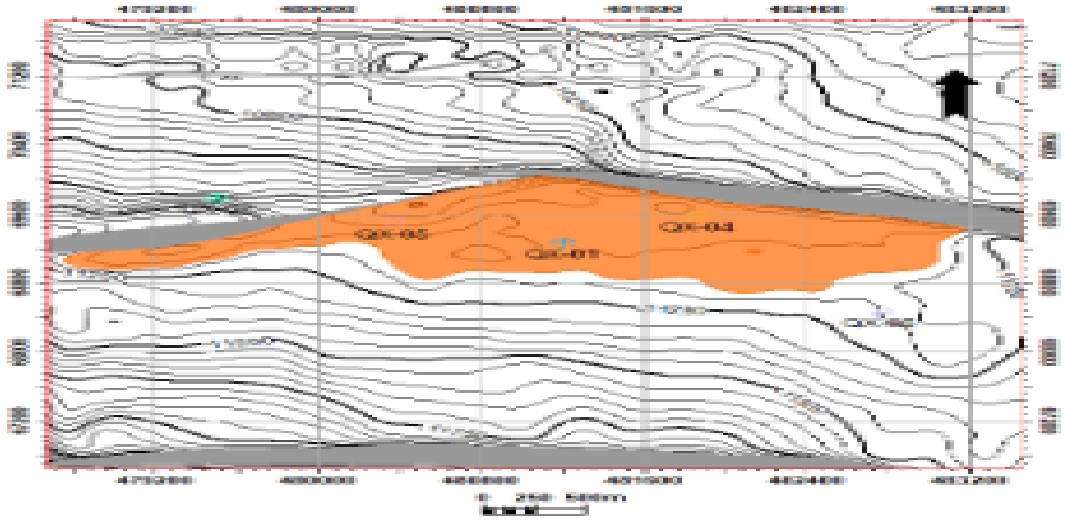

Figure 20: Depth structural maps for RES 3

Table 6: Result of the Volume Estimation

Reservoir	STOIIP (MMSTB)			GIIP (BCF)		
CASES	P10	P50	P90	P10	P50	P90
RES 1(MC)	9.20	6.13	3.07	4.68	2.66	1.33
RES 2(MC)	-	-	-	14.31	9.54	4.77
RES 3(MC)	87.41	58.27	29.14	-	-	-
TOTAL(Probabilistic)	93.90	64.40	35.10	17.26	12.20	7.14

This effect demonstrates that the overall uncertainty in a field's reserves is generally less than the sum of uncertainties in individual reservoirs, because extreme outcomes in different reservoirs are unlikely to occur simultaneously.

P50 (Best Estimate): The P50 value remains unchanged at 64.40 MMSTB, reflecting that the arithmetic mean (or median) of independent distributions aggregates linearly. This stability confirms that the best estimate of the field volume is robust against the method of aggregation. P10 and P90 (Uncertainty Range): The arithmetic sum approach produced an excessively wide range, from 32.21 MMSTB (P90) to 96.61 MMSTB (P10). Such a range implies a statistically unrealistic scenario where

all reservoirs simultaneously experience their extreme low or high volumes, overestimating both risk and opportunity.

The probabilistic aggregation corrects this distortion, yielding a narrower and more realistic uncertainty range of 35.10 MMSTB (P90) to 93.70 MMSTB (P10). This range appropriately accounts for the compensating effects across independent reservoirs: high volumes in one reservoir are likely offset by lower volumes in another, reducing overall uncertainty and providing a more accurate risk profile for field development planning.

Interpretation of Probabilistic Totals:
The P90 volume (35.10 MMSTB) represents the conservative or proved reserves, indicating a 90% probability that the field contains at least this volume. This metric is critical for planning safe and risk-mitigated development strategies.
The P10 volume (93.70 MMSTB) reflects the optimistic or possible reserves, suggesting only a 10% chance that the field volume will exceed this estimate. This figure helps management understand the upside potential while acknowledging its low probability. The probabilistic aggregation of Monte Carlo simulation outputs produces statistically robust volumetric estimates, providing a more reliable foundation for field development, economic evaluation, and risk assessment. By explicitly capturing the Portfolio Effect, this approach mitigates the overstatement of risk inherent in simple arithmetic summation and enhances confidence in the reported reserves.

4.9 Probabilistic Aggregation of Gas Initially In Place (GIIP)

The probabilistic aggregation of Gas Initially In Place (GIIP) employed the same rigorous methodology as used for STOIIP, ensuring consistency and statistical integrity across all hydrocarbon volume estimates. This approach allows for a realistic assessment of uncertainty and risk when evaluating the total gas potential of the field. Figure 22 illustrates the critical difference between the naïve arithmetic summation of individual reservoir volumes and the statistically corrected probabilistic aggregation. When the P10 and P90 values from each reservoir were added arithmetically, the resulting uncertainty envelope was exaggerated (P10: 18.99 BCF; P90: 6.10 BCF). This approach implicitly assumes that all reservoirs would simultaneously realize their extreme high or low volumes, a scenario that is statistically improbable - thus overstating both the potential upside and downside risk.

To address this according to Yang et al. (2023), the Variance Addition Method, commonly referred to as the Root-Sum-of-Squares (RSS), was applied. By assuming statistical independence between reservoirs, the RSS method more accurately aggregates uncertainties, resulting in a narrower and more realistic total GIIP range (P10: 17.26 BCF; P90: 7.14 BCF). This reduction in uncertainty illustrates the Portfolio Effect, whereby combining independent reservoirs mitigates overall risk and reduces the likelihood of extreme outcomes.

Key observations from this probabilistic aggregation include:
Improved confidence in minimum reserves: The P90 conservative estimate increased from 6.10 BCF to 7.14 BCF, indicating that the minimum expected gas volumes are slightly higher than previously suggested by arithmetic addition. This provides greater assurance for reserve planning and project economics. Moderation of extreme optimism: The P10 optimistic estimate decreased from 18.99 BCF to 17.26 BCF, highlighting that the likelihood of achieving the maximum possible gas volume is lower when uncertainties across reservoirs are considered collectively.

Recommendation for reporting: The final, accepted Total GIIP should be expressed probabilistically as 17.26 BCF / 12.20 BCF / 7.14 BCF (P10 / P50 / P90). This probabilistic representation accurately captures the combined uncertainty of the field, ensuring a more realistic

appraisal of both risk and opportunity (Akpan et al., 2022b).

Overall, this analysis demonstrates that probabilistic aggregation is essential for a credible assessment of field-wide gas volumes. By incorporating statistical principles and recognizing the independence of reservoir uncertainties, the resulting GIIP estimates provide a robust framework for decision-making and resource evaluation.

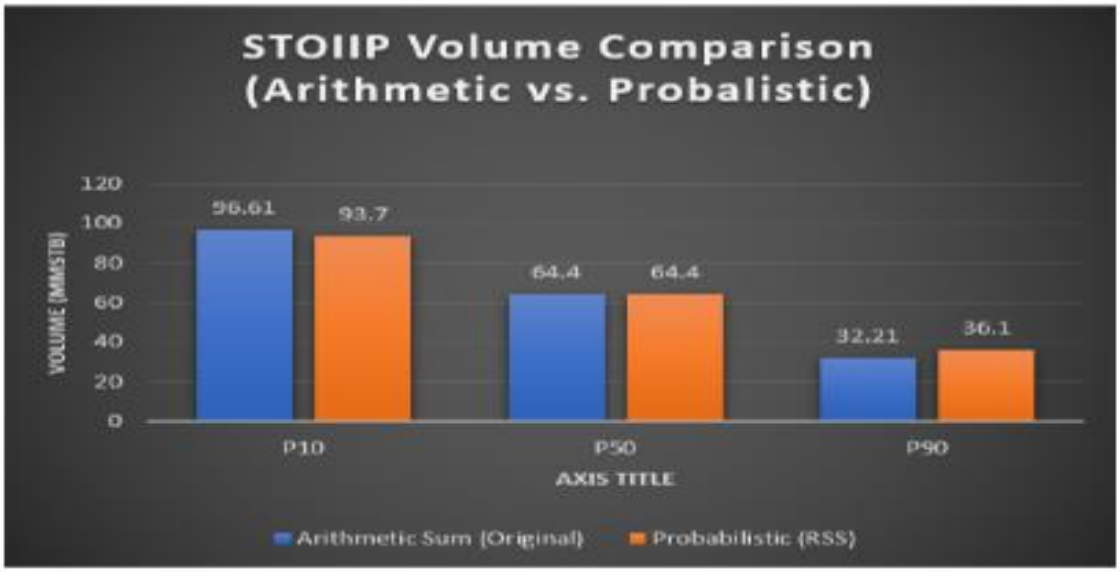

Figure 21: STOIIP Total Volume Comparsion

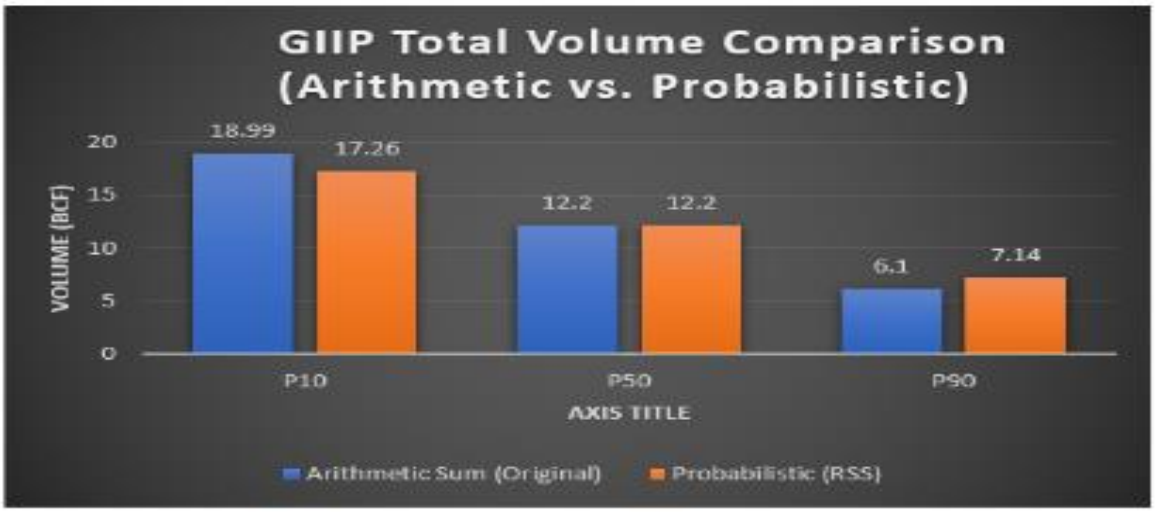

Figure 22: GIIP Total Comparsion

5.0 Conclusion

This study conducted a comprehensive qualitative and quantitative evaluation of the depositional environment and hydrocarbon prospectivity of the QX Field in the Southeastern Niger Delta. Analysis of the three delineated reservoir units (RES 1, RES 2, and RES 3) reveals distinct sedimentological characteristics, indicating deposition across a spectrum of deltaic settings, from channelized to lower shoreface environments. These depositional environments exerted a significant control on reservoir architecture, influencing lateral continuity, net-to-gross ratio, thickness variations, and petrophysical quality.

The integrated approach, combining lithofacies interpretation, petrophysical evaluation, and probabilistic volumetric analysis, highlights the heterogeneity and potential of each reservoir. RES 1 and RES 2 exhibit relatively higher net thicknesses and favorable petrophysical properties, suggesting superior storage capacity

and hydrocarbon productivity compared to the deeper RES 3. This spatial variation underscores the importance of depositional control in reservoir quality and the predictive value of sequence stratigraphic and sedimentological analysis in deltaic systems.

Furthermore, the application of a simplified probabilistic volumetric approach demonstrates a cost-effective methodology for assessing hydrocarbon potential while effectively accounting for uncertainties in reservoir parameters. This approach provides a robust decision-making framework for field development planning and investment risk reduction. Overall, the findings indicate that the QX Field possesses reservoirs with high hydrocarbon prospectivity, capable of economically producing both oil and gas. These results also offer valuable insights applicable to the evaluation of emerging marginal fields across the Niger Delta basin.

Acknowledgements

The authors sincerely acknowledge the Nigerian Upstream Petroleum Regulatory Commission (NUPRC) for providing access to the essential datasets and technical information that underpinned this study. Their support was instrumental in enabling a rigorous and comprehensive evaluation of the QX Field.

References

Adeoye, T.O, Enikanselu P (2009). Reservoir Mapping and Volumetric analysis using Seismic and Well Data. Ocean J. App. Sci. 2(4): 66 – 67

Aigbedion J. A, Iyayi, S E (2007). Formation Evaluation of Oshioka Field, using geophysical well logs Middle-east J. of Scientific Res. 2(3 – 4):107 – 110

Akpan, A. S., Obiora, D. N., Okeke, F. N., Ibuot, J. C., & George, N. J. (2020b). Influence of wavelet phase rotation on post stack model based seismic inversion: A case study of X-field, Niger Delta, Nigeria. Journal of Petroleum and Gas Engineering, 11(1), 57-67.

Akpan, A.S., Okeke, F.N., Obiora, D.N.& George, N.J. (2020a). Modelling and mapping hydrocarbon saturated sand reservoir using Poisson's impedance (PI) inversion: a case study of Bonna Field Niger Delta swamp Depobelt, Nigeria. J. Pet. Explor. Prod. Technol. Ger. 11 (117), 132. https://doi.org/10.1007-/s13202-020-01027-8.

Akpan, M. J., George, N. J., Ekanem, A. M., & Nathaniel, E. U. (2022a). Utilizing Probabilistic Neural Network for Reservoir Assessment: A Case Study from an Onshore Niger Delta Field. *Researchers Journal of Science and Technology*, *2*(3), 55–67. Retrieved from https://rejost.com.ng/index.php/home/article/view/41

Akpan, M.J., George, N.J., Ekanem, A.M. & Ekong, U.N., (2022b). Petrophysical appraisal and 3D structural interpretation of reservoirs in an Onshore Niger Delta Field, Southeastern Nigeria. Int. J. Energy Water Resour. https://doi.org/10.1007-/s42108-022-00218-9.

Allen, P.A. and Allen, J.R. (2005) Basin Analysis, Principles and Applications. Blackwell Publishing, Hoboken.

Archie, G. E. (1942). The Electrical Resistivity Log as an Aid in determining Some Reservoir Characteristics. Petroleum Transactions of the American Institute of Mining, Metallurgical and Petroleum Engineering (AIME), 146, 54–62.

Asquith, G., & Krygowski, D. (2004). Basic Well Log Analysis (2nd ed.). AAPG.

Burke, K. (1969). Longshore drift, submarine canyons, and canyons on the Niger Delta. Journal of Geology, 80(5), 539-550.

Burke, K., Dessauvagie, T. F. J., & Whiteman, A. J. (1971). Opening of the Gulf of Guinea and geological history of the Benue Depression and Niger Delta. Nature Physical Science, 233(39), 51-55

Castro, C. C., Hámor-Vidó, M., Geiger, J., Kovács, J., & Fedor, F. (2026). Textural and Petrophysical Controls on Reservoir Quality: Insights from the Szentes Geothermal Field, Hungary. *Energies*, *19*(7), 1688. https://doi.org/10.3390-/en19071688

Chopra, S., & Marfurt, K. J. (2007). Seismic Attributes for Prospect Identification and Reservoir Characterization. Society of Exploration Geophysicists (SEG) Publications

Dake, L. P. (1978). Fundamentals of Reservoir Engineering. Elsevier.

Daukoru, C. M. (1994). Northern Delta Depobelt Portion of the Akata-Agbada Petroleum system, Niger Delta, Nigeria. Petroleum Association System, AAPG memoir 60. American Association of Petroleum Geologists (AAPG), Tulsa, 598–616.

Doust, H., & Omatsola, E. (1990). Niger Delta. In J. D. Edwards & P. A. Santogrossi (Eds.), Divergent/Passive Margin Basins: AAPG Memoir 48. American Association of Petroleum Geologists, Tulsa, 48, 239–248.

Downey, J. D. (2005). Seismic sequence stratigraphy: Recent advances and applications. In J. R. Boles & T. M. Bown (Eds.), Geological Society of America Special Paper 392: Applied Stratigraphy: From Pre-Feldspar to Hydrocarbon Exploration (pp. 1–20). Geological Society of America.

Ebong, S. T., Ekanem, A. M., & George, N. J. (2023a). Reservoir Characterization Using Seismic Inversion Techniques for Mapping of Prospects. *Researchers Journal of Science and Technology*, *3*(1), 1–13.

Ebong, S.T., Ekanem, A.M. & George, N.J. (2023b). Fluid Prediction Through Lithological Analysis in 'M' Oil Field Niger Delta: Using Rock Physics Approach. Earth Sciences Malaysia, 7(1): 55-61.

Ekanem, A.M., George, N.J., Thomas, J.E. Ekpenyong, N.E. (2021). Seismic modelling study of CO_2 effects on P-wave amplitude. *Model. Earth Syst. Environ.* **7**, 1693–1701 (2021). https://-doi.org/10.1007/s40808-020-00904-9

Ekefre, A. E., George, N. J., Udoh, A. C., Harry, T. A., & Etim, C. E. (2025). Predictive Analysis of Sand Production and Flow Implications using Petrophysical-Geomechanical Properties: A case of "ANY" Field, Niger Delta. *Researchers Journal of Science and Technology*, *5*(2), 54–73.

Ekong, S. U., George, N. J., Udoh, A. C., & Ekefre, A. E. (2025). Integrated Reservoir Characterization and Bypassed Hydrocarbon Evaluation for Optimized Recovery in 'UDEN' Field, Niger Delta, Nigeria. *Researchers Journal of Science and Technology*, *5*(7), 67–84. Retrieved from https://rejost.-com.ng/index.php/home/article/view/227

Emujakporue, G.O, Faluyi T.O (2015). Evaluation of hydrocarbon volume in'TRH' Field, onshore Niger Delta, Nigeria. Int. J. Geophy and Geochem. 2(5):113 - 123.

Etim, C. E., Bassey, N. E., Harry, T. A., & Ekefre, A. E. (2026). Integrated Log-Derived Geomechanical Characterization and Sand Production Prediction for Sand Management in the EL Field, Niger Delta. *Researchers Journal of Science and Technology*, *5*(8), 31–65. Retrieved from https://rejost.com-.ng/index.php/home/article/view/231

García-Gutiérrez, M., Mingarro, M., Morejón, J., Alonso, U., & Missana, T. (2023). Analysis of the Role of Water Saturation Degree in HTO, ^{36}Cl, and ^{75}Se Diffusion in Sedimentary Rock. *Minerals*, *13*(5), 593. https://doi.org/10.3390/min13050-593

Kulke, H. (1995). In H. Kulke (Ed.), Regional Petroleum Geology of the World. Part II: Africa, America, Australia and Antarctica. Gebrüder Borntraeger, pp. 143–172.(Oloruntobi, A. (1997). Prospecting for Hydrocarbon in Niger Delta region, Mobil News January, 1997. 13p.

Ma, M., Lin, C., Liu, Y., Li, H., Yuan, W., Liu, J., Shi, C., Zhang, M., & Xu, F. (2025). Depositional Evolution and Controlling Factors of the Lower–Middle Jurassic in the Kuqa Depression, Tarim Basin, Northwest China. *Applied Sciences*, *15*(14), 7783. https://doi.org/10.3390-/app15147783

Meng, L., Shi, X., Yang, W., Zhang, C., & Xu, W. (2023). Study on the Evaluation Method of the Water Saturation Logging of a Low-Resistance Oil Reservoir in the Guantao Formation, Bohai Basin. *Processes*, *11*(10), 2890. https://doi.org/-10.3390/pr11102890

Olowokere, M. T., Hassane, A., Alonge, M. A., & Ajibade, E. A. (2019). Hydrocarbon prospectivity determination of "eagle field", coastal swamp ii Niger delta. International Journal of Advanced Geosciences, 7(1), 52-57.

Short, K. C., & Stauble, A. J. (1967). Outline of Geology of Niger Delta. American Association of Petroleum Geologists, Bulletin, 51, 761–779.

Slatt, R. M. (2006). Stratigraphic Reservoir Characterization for Petroleum Geologists, Geophysicists, and Engineers. Elsevier.

Society of Petroleum Engineers (SPE). (2018). Petroleum Resources Management System (PRMS). SPE, World Petroleum Council, American Association of Petroleum Geologists, Society of Petroleum Evaluation Engineers, Society of Exploration Geophysicists, Society of Petrophysicists and Well Log Analysts, and Latin American and Caribbean Petroleum Engineering Confederation.

Stacher, P. (1995). Present understanding of the Niger delta hydrocarbon habitat. In M. N. Oti & G. Postma (Eds.), Geology of Deltas. A. A. Balkema, Rotterdam, pp. 257–267

Tearpock, D. J, Bischke R.E. (2003). Applied subsurface geological mapping with structural methods. 2nd, Edition. Prentice Hall, PTR, Upper saddle, River, New Jersey.

Tuttle, M. L., Charpentier, R. R., & Brownfield, M. E. (1999). The Niger delta Petroleum System: Niger delta Province, Nigeria, Cameroon, and Equatorial Guinea,

Africa (pp. 99–50). US Department of the Interior, US Geological Survey.

Udo, K. I., George, N. J., Akankpo, A. O., Azuoko, G. B., & Aka, M. U. (2020). Determining fracture pressure gradients from well logs. *Int J Adv Geosci*, *81*(1), 5-9.

Udoinyang, I.E., Akpan, E., & N. J. George. (2019) Petrophysical Application towards Achieving Optimum Secondary Recovery in Heterogeneous Reservoirs, Journal of Geography, Environment and Earth Science International 23(4): 1-9

Uzuakpunwa, A.B. (1974) The Abakaliki pyroclastics Eastern Nigeria New age and tectonic implications Geological Magazine 111 1 65-70

Walker, R. G. (19792). Deep-water sandstone facies and ancient submarine fans: models for exploration for stratigraphic traps. AAPG Bulletin, 62(6), 932–966.

Weber, K. J., & Daukoru, E. M. (1975). Petroleum geology of the Niger Delta. Proceedings of the Ninth World Petroleum Congress, 2, Geology: Applied Science Publishers, Ltd., London, pp. 210–221.

Whiteman, A. J. (1982). Nigeria: Its petroleum geology, resources and potential. London, Graham and Trothman, 1:166.

Xu, Z., Zheng, B., Liu, B., & Song, W. (2025). Stratigraphic Correlation of Well Logs Using Geology-Informed Deep Learning Networks. *Processes*, *13*(5), 1288. https://doi.org/10.3390/pr13051288

Yang, J., Bai, G., & Yan, M. (2023). Minimum Residual Sum of Squares Estimation Method for High-Dimensional Partial Correlation Coefficient. *Mathematics*, *11*(20), 4311. https://doi.org/10.3390-/math11204311